

**MODELING, ANALYSIS, AND SIMULATION OF TEMPERATURE-
DEPENDENT FLUCTUATIONS IN THE POPULATION OF THE
YELLOW FEVER MOSQUITO, *AEDES AEGYPTI*, IN OUTDOOR,
INDOOR, AND UNDERGROUND HABITATS**



Annika Roise

Professor Dorothy Wallace, Advisor

Department of Mathematics
Dartmouth College
Hanover, NH

May 2018

Acknowledgements

First and foremost, I would like to thank my advisor, Professor Dorothy Wallace, for guiding my research over the last two years. This project would never have been possible without her patience, dedication, and encouragement, and I am grateful for the many hours she devoted to making this process incredibly educational and fulfilling. In addition to Professor Wallace, I extend my gratitude to all of my math professors at Dartmouth, and to the Office of Undergraduate Advising and Research, for funding the first two terms of this project through the Presidential Scholars program. I would also like to thank my friends and colleagues in the math department, Jacob Savos '16 and Evan Rheingold '17, for offering their advice and MatLab expertise in the early stages of developing this model. Finally, I would like to thank the friends on campus who have supported me through this project's completion, and my parents, for encouraging me to never stop pursuing my love of math.

Abstract

Aedes aegypti, also known as the yellow fever mosquito, is a mosquito of African origin that transmits dengue fever, Zika virus, yellow fever, and chikungunya. The diseases associated with the vector have generated increasing international concern in recent years, with more than one-third of the world's population now living in regions that are susceptible to infection. Many of the illnesses that *Aedes aegypti* transmits still lack a cure or vaccine, and transmission is best controlled through the prevention of human-mosquito contact and the monitoring of the vector population. In this study, we develop a model for the *Aedes aegypti* lifecycle in the interest of understanding the viability of its survival in manmade environments in several major U.S. cities. We propose a system of ordinary differential equations describing the vector's growth from egg to adult that accounts for habitat heterogeneity by incorporating migration among outdoor, indoor, and underground habitats. Based on an analysis of the existence of population equilibria at a range of temperatures, we select six U.S. cities whose climates represent differing levels of suitability for the vector's survival. We validate our results against the reported range of *Aedes aegypti* in the United States and confirm that the presence of climate-controlled habitats leads to potential viability in regions in which vector survival was not previously considered feasible.

Contents

1. Introduction	1
2. The Model	11
2.1 Equations	12
2.1.1 Outdoor Habitat Modifications	14
2.1.2 Indoor Habitat Modifications	15
2.1.3 Enclosed Habitat Modifications	16
2.1.4 Complete System of Habitat-Specific Equations	17
2.2 El Paso Climate	18
2.2.1 Outdoor Temperature	18
2.2.2 Indoor Temperature	18
2.2.3 Enclosed Temperature	19
2.3 Lifecycle Parameters	20
2.3.1 Egg Production Rates	20
2.3.2 Egg Flooding and Hatching Rates	21
2.3.3 Egg Death Rates	22
2.3.4 Maturation Rates for Larvae and Pupae	22
2.3.5 Temperature-Dependent Death Rates for Larvae and Pupae	23
2.3.6 Density-Dependent Death Rates for Larvae	24
2.3.7 Adult Transition and Death Rates	25
2.3.8 Migration Rates	27
3. Model Analysis and Equilibrium Viability	31
4. Methods	35
4.1 Modeling Habitat Variations	35
4.2 Comparing Outdoor Survival Among Regions	37
4.3 Evaluating the Impact of Indoor Habitat	39
5. Results	41
5.1 Habitat Balance	41
5.2 Outdoor Viability by Region	46

5.3 Effects of Indoor Habitat Re-Introduction	51
6. Discussion	55
7. References	59

1. Introduction

Aedes aegypti is a mosquito of African origin that transmits several vector-borne illnesses of international concern, which include dengue fever, Zika virus, yellow fever, and chikungunya. The vector begins as an egg and matures through multiple aquatic life stages before reaching adulthood, during which maturation and mortality rates are temperature-dependent (Tun-Lin et al. 2000). In the absence of manmade habitat, the vector's survival is contingent on the presence of appropriate outdoor temperature conditions. However, the preference of *Aedes aegypti* for feeding on human hosts most often leads the vector to occupy regions in which buildings, water-filled manmade containers, and underground infrastructure provide temperature and wetness conditions that are more conducive to survival than naturally occurring habitats (Ritchie et al. 2013). Beyond understanding the geographical range in which *Aedes aegypti* can survive outdoors, analyzing the scope of its viability in the presence of manmade habitats is an essential means of informing preventative measures against vector spread and disease transmission.

The illnesses associated with *Aedes aegypti* cause varying symptoms in infected individuals and have appeared in broad portions of the world's area. Yellow fever outbreaks took place in Europe and the Americas for centuries before the infection's link with *Aedes aegypti* was confirmed in 1900. While vaccines for the illness are now widely distributed, reducing long-term transmission risk, hundreds of cases are still reported annually in South America and Africa. Symptoms of yellow fever range from minor aches to severe liver disease, for which there exists no medical cure or treatment ("Yellow Fever"). Yellow fever is unique among the infections transmitted by *Aedes aegypti* in that its prevalence in the United States is extremely low; no cases have been reported in the continental United States in recent years and the last local outbreak took place in the early 20th century. However, the illness remains a public health threat in many of the world's developing nations.

Dengue fever is endemic in Puerto Rico, South America, and Southeast Asia, and has appeared in sporadic outbreaks in the continental United States over the last two decades. Between 1999 and 2010, outbreaks took place in Miami and Key West, Florida, as well as in two Texas cities along the Mexican border. Several locally transmitted cases have since been reported in both Texas and southern Florida ("Dengue"). Dengue is recognized as the fastest-

spreading mosquito-borne illness in the world, and it stands to affect a growing portion of the United States in the coming years (Bouri et al. 2012). Chikungunya has followed a similar timeline in the United States, with few diagnoses taking place prior to 2006. Local transmission was first identified in Florida in 2014 after several years during which the infection arose exclusively in travelers returning from Asia, Africa, and Latin America (“Chikungunya”). The recent footholds of both dengue and chikungunya in the United States indicate a risk of further spread in the absence of additional vector management.

Zika virus was first isolated in Uganda in 1947, but few cases were reported until 2007, when the first large outbreak occurred on the island of Yap, Federated States of Micronesia. By 2015, outbreaks had taken place in several additional groups of Pacific islands and seven South American nations. In Brazil, where thousands of mild cases of Zika virus were reported, researchers noted an increase in the prevalence of the neurological disorder Guillan-Barré Syndrome, the majority of which were associated with Zika infection. The World Health Organization (WHO) declared Zika virus a Public Health Emergency of International Concern in early 2016 based on the disease’s apparent association with the birth defect microcephaly and other neurological disorders (“Zika Virus Fact Sheet”).

The first cases of Zika virus in the mainland United States appeared in February 2016, when two sexually transmitted cases were reported in Texas. While both cases were introduced by individuals who had traveled to the U.S. from other affected countries, by July of the same year, four locally transmitted cases had been confirmed in Miami. As of April 2018, the Centers for Disease Control and Prevention (CDC) has reported 5,676 total symptomatic cases of Zika virus in U.S. states, 229 of which are presumed to have been transmitted through local vectors (“Zika Virus”). Although vector population levels cannot be fully conflated with disease risk, analyzing the current and future viability of *Aedes aegypti* survival in the continental United States remains a means of designating the regions with greatest potential for the future spread of these infections.

Given the persistent risk of vector survival and disease transmission in the United States, this study examines the *Aedes aegypti* population’s response to annual weather fluctuations and evaluates the effects of habitat variability under the assumption that the vector primarily occupies manmade receptacles. We begin our analysis of temperature-dependent population dynamics using climate data from El Paso, TX, a region close to the initial arrival site of Zika

virus and dengue fever, which remains at risk for *Aedes aegypti* breeding and dispersal. Beyond El Paso, we analyze annual survival viability in Minneapolis, MN, New York, NY, New Orleans, LA, Orlando, FL, and Miami, FL. These regions, which range from humid continental climates with cold winters to tropical regions with year-round warm temperatures, are each considered to present a distinct risk level for *Aedes aegypti* survival and disease transmission (Monaghan et al. 2016).

In addition to the natural climate conditions that make the survival of *Aedes aegypti* adults viable for some or all of each year in each of the aforementioned cities, habitat heterogeneity is a central factor in vector survival and an essential consideration for the development of control strategies. In cities and suburbs with ample manmade infrastructure, the vector migrates freely among outdoor areas, buildings, and enclosed spaces such as water tanks, water towers, and underground sewage systems as it searches for feeding subjects and oviposition sites. While outdoor environments are exposed to a region's full range of weather patterns, climate-controlled indoor environments are kept at constant temperatures, and enclosed or underground areas are sheltered to some degree from exterior conditions (Russell et al. 2001). In this study, we consider a separate set of temperature conditions to govern each of these habitat types and adjust the balance among them to explore the possibility of vector population reduction through habitat cleanup and control.

Our model expands upon preexisting studies of *Aedes aegypti* population dynamics by synthesizing information from existing models with specific characteristics of the regions and habitat types of interest. An early *Aedes aegypti* lifecycle model was proposed by Bar-Zeev, who investigated the effects of temperature on growth and survival of premature mosquitos. As a basic relationship between temperature and the rate of *Aedes aegypti* development, Bar-Zeev proposed the equation $t(T - c) = K$, where t represents development duration, T is temperature, c is the development threshold, and K is a constant. This equation suggests an inverse relationship between development time and temperature and reflects Bar-Zeev's observation that the duration of larval development decreased incrementally as temperature rose from 16°C to 36°C (Bar-Zeev 1958). However, the model fails to differentiate between maturation patterns at different life stages and to capture temperature-independent factors, such as population density, that are influential to development and survival (Barbosa et al. 1972). Furthermore, the model

does not consider habitat characteristics, such as the proportions of available wet and dry egg-laying areas, that affect *Aedes aegypti* prevalence (Sota and Mogi 1992).

Dye proposed a subsequent comprehensive model of *Aedes aegypti* population dynamics that expresses changes in the adult population as an exponential function. In this study, the rate of change of the number of *Aedes aegypti* adults at time t is expressed as $\frac{dA(t)}{dt} = PA(t - T)\exp[-\alpha(A(t - T)E)^\beta] - \delta A(t)$, a function of daily egg production less a daily adult death rate. Dye's equation is based on a lifecycle structure that includes eggs, four larval stages, pupae, and two groups of adults: feeding and egg-laying. The model facilitated Dye's study of the size and stability of the adult population at equilibrium, which accurately reproduced the equilibrium dynamics of a laboratory population previously studied by Gilpin (Dye 1984; Gilpin et al. 1976). However, like Bar-Zeev, by simplifying the lifecycle model to an expression of the rate of change of the adult population, Dye excludes an analysis of fluctuations in other life stages that would be useful to understanding overall population dynamics. Additionally, while the model includes a parameter describing density-dependent mortality, it does not account for habitat characteristics such as temperature and wetness that also affect vector development and survival (Ermert et al. 2011).

We also draw on the Container-Inhabiting Mosquito Simulation Model (CIMSIM) developed by Focks, which remains a fundamental model for *Aedes aegypti* development. More intricate than Bar-Zeev and Dye's models, CIMSIM accounts for the effects of temperature, density, and habitat heterogeneity on mosquitos in each life stage. The study is based on observations of *Aedes aegypti* maturation in nine different containers with varying conditions. In addition to total development rate, it describes size, fecundity, and the gonotrophic cycle, and takes in separate parameters for larval and pupal development. The resulting system of equations relates temperature with development rate, survival, and larval weight change, and is validated through comparison with the results of field studies in Thailand (Focks et al. 1993). In addition to the factors represented in Bar-Zeev's equation, the model accounts for varying habitat types and the effects of temperature on characteristics beyond maturation rate. However, Focks' model does not consider distinct temperature models to govern different habitat types, nor does it account for migration or oviposition in dry habitats.

Yang proposed an additional temperature-dependent model of the *Aedes aegypti* lifecycle that investigates mortality, life stage transitions, and oviposition at different temperatures. Yang

models *Aedes aegypti* fluctuation through a system of two differential equations that describe the rate of change of the aquatic population and the adult population. Changes to the aquatic population are modeled as a function of oviposition rate and carrying capacity less emergence and mortality, while the adult population fluctuates as a function of the difference between emergence and adult mortality rates. Based on this model, Yang solves for two points at which the population reaches equilibrium, one of which is trivial and the other a function of the mean number of female offspring produced by a female during her life (Yang et al. 2009). Yang's treatment of maturation as a system of differential equations and subsequent investigation of equilibrium points are similar in format to our study of *Aedes aegypti* prevalence. Nevertheless, our model expands upon Yang's study by considering multiple habitats and aquatic stages, as well as density-dependent parameters.

Last among comprehensive *Aedes aegypti* population models, this study considers Skeeter Buster, a stochastic modeling tool developed by Magori et al. that builds upon Focks' CIMSIM approach by incorporating mosquito genetics and a new set of habitat types. Skeeter Buster evaluates fluctuations in the vector population at the individual container level, accounting for spatial dynamics through migration among specifically defined properties. At each of the life stages in the model, which include eggs, one larval group, pupae, and adults, an algorithm based on survival probabilities determines survival and transition into the next stage. The authors show that habitat heterogeneity influences both genetic makeup and population density (Magori et al. 2009). Skeeter Buster's incorporation of climate data to predict population levels facilitates the demarcation of the vector's range of viability in the United States (Monaghan et al. 2016). Nevertheless, several characteristics of our model differ from Magori's approach. First, while Skeeter Buster indicates habitat variability through the consideration of distinct properties and container sizes, we establish three habitat types governed by separate climate conditions to analyze the temperature-dependent effects of habitat heterogeneity. We account for more life stages, including dry eggs and multiple larval and adult subgroups, and determine transitions among them using a system of differential equations rather than a stochastic model. Finally, we consider migration as determined by the distribution of available aquatic habitat and human subjects rather than dispersal probabilities.

Our lifecycle model also reflects approaches to modeling similar vectors and diseases, one of which is a revision of the Liverpool Malaria Model by Ermert et al. Ermert and his

collaborators evaluate malaria transmission dynamics as affected by temperature and precipitation, acknowledging that malaria is a water-associated disease that is most prevalent in warm and humid climates. The model includes three aquatic stages and a gonotrophic cycle occurring during the adult stage, as well as a disease transmission interaction between adult mosquitos and humans. Parameters are weather-dependent, and include the number of humid and dry days, the number of eggs produced, daily survival, temperature thresholds, and transmission characteristics. Ermert's model simulates the daily spread of malaria based on mean temperature and accumulated rainfall (Ermert et al. 2011). The treatment of survival and maturation as dependent on temperature and wetness is similar to our model's considerations; however, we examine the aquatic stages in more detail and choose parameters to reflect the conditions of *Aedes aegypti* by region and habitat type.

This paper is most similar in structure to a model that Wallace et al. developed to represent the population of *Anopheles gambiae*, the Malaria vector. Wallace models the population using a system of seven ordinary differential equations that reproduce emergence rates and instar ratios observed in the Kenya Highlands. The equations describe population changes for eggs, four larval stages, pupae, and adults. Each represents the rate of change as maturation from the previous stage less maturation into the following stage and up to two death terms (Wallace et al. 2017). Our model for the *Aedes aegypti* population mirrors Wallace's fundamental approach to representing maturation and death rates, but it includes several modifications based on differences between the two vectors. For *Aedes aegypti*, eggs laid in wet and dry locations are considered separately, as eggs are known to survive in both environments (Sota and Mogi 1992). We use two distinct equations to model fluctuations in the populations of feeding and laying adults and account for differences in migration preferences among these groups. Transitions back and forth between the two adult stages are also included to reflect the distinct multiple feeding and laying tendencies of *Aedes aegypti* (Klowden and Briegel 1994; Pant and Yasuno 1973). Finally, habitat parameters are modified to reflect the conditions of outdoor, indoor, and enclosed areas. While our model recalls aspects of the *Anopheles gambiae* study as well as previous equations for *Aedes aegypti*, it takes in additional evidence from the literature to more closely reflect the vector's lifecycle in the United States.

Information on temperature-dependent maturation and death rates is derived primarily from a study by Tun-Lin, who observed larval development in Queensland, Australia and

documented the duration of each life stage through both laboratory and field studies. Tun-Lin found that no mosquitos survived at 10°C or 40°C, while survival and development rates both peaked around 25°C (Tun-Lin et al. 2000). Tun-Lin's findings facilitate our modification of maturation and death rates in Wallace's *Anopheles gambiae* model to reflect the lifecycle of *Aedes aegypti*. Information on development and survival rates is also provided by Rueda, who observed the development of *Aedes aegypti* mosquitos reared at various temperatures in laboratory and compared the results to predictions from the Sharpe & DeMichele four-parameter temperature-dependent model for poikilotherm development (Rueda et al. 1990; Sharpe and DeMichele 1977). Rueda's reports of the duration of development at each temperature are close in value to both Sharpe and DeMichele's predictions and Tun-Lin's observations. We refer to Tun-Lin's exact counts, as these results are validated in the field as well as in laboratory.

In addition to incorporating Tun-Lin and Rueda's findings on larval and pupal development, we model development patterns for the egg stage based on a study by Sota and Mogi, who recorded survival times of eggs at various humidity levels. Sota and Mogi's study affirms that survival time is correlated with population density and habitat availability in addition to temperature in the aquatic stages (Sota and Mogi 1992). For a further understanding of mosquito growth within a finite habitat, we refer to Southwood, who proposed a life budget model based on daily counts of *Aedes aegypti* in each life stage in Wat Samphaya, Thailand. Southwood surveyed the households and water receptacles in a confined area and took mosquito counts to calculate development rates based on the number of days since a flooding event (Southwood 1972). Southwood's daily counts of the population in each life stage provide a means of estimating the proportion of the population falling in each subgroup at equilibrium. We validate our model's equilibrium results against Southwood's reported emergence rates and instar ratios.

Studies by Barbosa and Moore reaffirm the importance of considering density-dependent development parameters. Barbosa observed eggs in a laboratory at eight different density levels and investigated differences in their weights and survival rates. High-density groups demonstrated stress effects, such as higher mortality and lower adult weight, as a result of lessened food availability during overcrowding. Barbosa found that crowding had a non-linear effect on survival rates, affirming our adoption of quadratic density-dependent death rates from the *Anopheles gambiae* model (Barbosa et al. 1972; Wallace et al. 2017). In another study of

larval density, Moore observed the production of growth retardant factors (GRF) in a colony in Puerto Rico with varying density and nutrition levels. Moore concluded that nutrition, not density, influences the production of GRF, implying that the density-dependent factors for which our model accounts are primarily physical rather than chemical (Moore et al. 1972). Based on findings from these two studies, we consider the density-dependent death rate as a grouping of the combined effects of predation and crowding.

Beyond the calculation of maturation and death rates, evidence from the literature informs our representation of the gonotrophic cycle. An early study of *Aedes aegypti* feeding and reproduction comes from Judson, who observed the oviposition behavior of a cohort of mosquitos raised in laboratory. Judson found that biting and oviposition typically took place in a nine-day cycle during which peak feeding rates occurred on days one, four, and seven, and egg-laying occurred on days three and six (Judson 1967). Our model replicates Judson's observation of two oviposition cycles by showing that half of the egg-laying adults return to the feeding stage each day for an additional round of oviposition. Judson's report also claims that feeding patterns differ between gravid and non-gravid mosquitos. However, for our model, we assume that all adult females are mated and gravid based on confirmation from Doug Watts, a researcher at the Mosquito Ecology and Surveillance Laboratory in El Paso (Watts 2017).

Subsequent studies of the gonotrophic cycle come from Pant and Costa. Pant used the mark-release recapture method to observe mating, feeding, and oviposition in the field in Thailand. Like Judson, he found that most mosquitos underwent two oviposition cycles, with about a three-day interval between them. Pant also observed seasonal fluctuations in biting and egg-laying rates based on temperature and wetness (Pant and Yasuno 1973). Costa's study of the gonotrophic cycle quantifies these effects by reporting oviposition rates in cohorts raised in six different temperature and humidity combinations. Costa found that when extremely high temperatures were paired with dry conditions, egg production and survival rates decreased. The time period during which females laid eggs was longest at 25°C, while females laid the most eggs per day at 30°C (Costa et al. 2010). In our model, Costa's findings are used to create temperature-dependent functions for the length of the gonotrophic cycle and the number of eggs laid per day.

We conclude our literature review with an overview of the sources describing common *Aedes aegypti* habitats. Barrera conducted a study using pupal counts from various containers in

Puerto Rico to determine the containers from which *Aedes aegypti* adults most commonly emerged. Using a cluster analysis to show aggregated mosquito distribution, Barrera concluded that the largest populations of pupae were found in unattended, rain-filled containers in yards. Barrera's findings suggest that *Aedes aegypti* control is best achieved by managing these household containers, and that wet outdoor containers are a primary habitat type to consider in our model (Barrera et al. 2006). Evidence for the enclosed outdoor environment comes from Burke et al. Burke studied septic tanks in Puerto Rico to show the relationship between mosquito prevalence and physical characteristics of a tank, such as surface area, cracks in the sides, and total dissolved solids. While Burke concluded that the presence of resting mosquitos in a septic tank does not necessarily mean they developed there, his description of these tanks as a viable habitat validates our consideration of enclosed and underground habitats (Burke et al. 2010).

Ritchie and Troyo studied urban habitats to form estimates of the total size of the adult *Aedes aegypti* population, as well as the areas mosquitos are most likely to inhabit. Ritchie released a group of mosquitos in Queensland, Australia and compared numbers of trapped mosquitos before and after release to estimate the size of the total mosquito population relative to the released population. In addition to deriving a total population count for Queensland, Ritchie indicated that *Aedes aegypti* mosquitos are most prevalent in urban areas (Ritchie et al. 2013). Similarly, Troyo surveyed a region in Costa Rica and characterized habitats by setting, type, and capacity. Troyo determined that over 80% of larval habitats were found on household lots, with domestic animal drinking containers, washtubs, and manholes among the most common environments (Troyo et al. 2008). These studies of *Aedes aegypti* breeding sites affirm the three broad habitat categories that we consider for vector development: Animal drinking containers and washtubs can be found either indoors or outdoors, and the presence of adult mosquitos in manholes justifies the consideration of an enclosed habitat category.

Based on findings from these studies, this paper synthesizes information on *Aedes aegypti* maturation, survival, and oviposition into a lifecycle model that accounts for heterogeneity and migration among manmade habitats in the U.S. cities of interest. While previous reports on the vector have described portions of its lifecycle, this model provides a detailed representation that differentiates between more life stages, habitat types, and factors influencing maturation than other studies. In Section 2 of the paper, we develop a system of ordinary differential equations describing the *Aedes aegypti* lifecycle and explain the derivation

of constant and temperature-dependent maturation and mortality parameters from the literature. In Section 3, we solve this model at equilibrium to report a range of temperatures at which the vector population can viably reach a constant level. In Sections 4 and 5, we explain our methods and the results of several numerical simulations that describe the effects of habitat variability and regional weather patterns on vector prevalence. Finally, in Section 6, we present our conclusions.

2. The Model

Our model consists of a system of ordinary differential equations describing population dynamics for eight stages of the *Aedes aegypti* lifecycle: dry eggs, wet eggs, two larval groups, pupae, and three adult groups. The model accounts for mosquitos appearing in three major habitat types: outdoors, indoors, and in spaces such as sewers and water tanks, which we will subsequently refer to as enclosed habitats. To represent the differences in maturation patterns that arise as a result of varying temperature and wetness among these spaces, we include three iterations of our system of differential equations where each is controlled by temperature and wetness patterns specific to one habitat. Transitions within habitats show maturation from one life stage to the next; transitions between habitats represent migration among physical environments. Figure 1 shows the interactions between components in the model. Biological transitions, which include maturation and egg-laying, are shown in solid arrows, while dashed arrows represent physical transitions such as flooding events and migration between habitats.

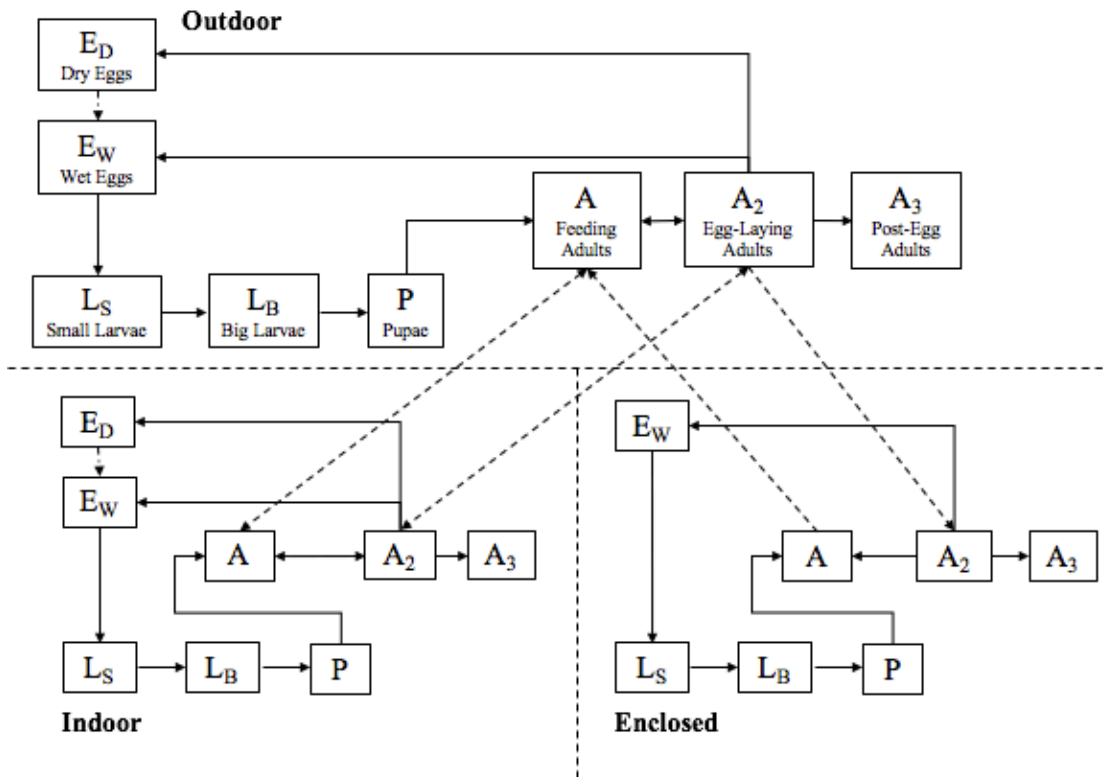


Figure 1. Flow diagram for the vector lifecycle. As explained above, each box represents one of eight life stages in one of three habitats. Solid arrows represent biological transitions such as maturation, while dashed arrows represent flooding and migration. The model is described by the system of ordinary differential equations specified in Equations (1) to (8).

In this section, we provide an overview of the system of equations as depicted above, explain the assumptions governing the three habitat types, and show the derivation of parameter values for these equations and habitats. Section 2.1 describes the aspects of the eight ordinary differential equations that are shared among all habitats, followed by the modifications that reflect migration and habitat heterogeneity. Section 2.2 explains our climate models, initially derived for El Paso, TX, which underpin the temperature-dependent parameters in the model and vary by habitat. In Section 2.3, we use data from previous studies to derive lifecycle parameters.

2.1 Equations

Within each of the three habitats, we represent fluctuations in the eight life stages using a system of ordinary differential equations. Terms in these equations align with the arrows showing transitions between life stages in the above diagram. Generally, the population in each stage increases as a result of maturation from the prior stage or migration from another habitat and decreases as a result of maturation into the next stage, migration out of the habitat, or death.

The rate of change of the dry egg population is expressed as the laying rate of eggs in dry places—the proportion of eggs laid in dry habitats ($1 - p_w$) times the number of eggs laid daily per female (e_b) times the number of egg-laying adult females (A_2)—less transition into the wet egg stage via flooding (n_{Ed}), and death (q_{Ed}).

$$(1) E_d' = (1 - p_w)e_b A_2 - n_{Ed} E_d - q_{Ed} E_d$$

The rate of change of the wet egg population is expressed as the sum of the laying rate of eggs in wet places ($p_w e_b A_2$) and the flooding rate of dry eggs (n_{Ed}), less hatching (n_{Ew}) and death (q_{Ew}).

$$(2) E_w' = p_w e_b A_2 + n_{Ed} E_d - n_{Ew} E_w - q_{Ew} E_w$$

The rates of change of the small and big larval populations are expressed as the hatching rate of wet eggs (n_{Ew}) and the maturation rate of small larvae (n_{Ls}), respectively, less maturation into the subsequent stage (n_{Ls}, n_{Lb}), a linear temperature-independent death rate (f_s, f_b), and a quadratic density-dependent death rate (q_{Ls}, q_{Lb}).

$$(3) L_s' = n_{Ew} E_w - (f_s + n_{Ls}) L_s - \frac{q_{Ls}}{k} L_s^2$$

$$(4) L_b' = n_{Ls} L_s - (f_b + n_{Lb}) L_b - \frac{q_{Lb}}{k} L_b^2$$

The rate of change of the pupal population is expressed as maturation from big larvae (n_{Lb}), less maturation into the first adult stage (n_p) and death (f_p).

$$(5) P' = n_{Lb}L_b - (f_p + n_p)P$$

Within the adult stages, population levels are determined by migration among habitats in addition to maturation and death. In this equation overview, we discuss only the maturation and death factors that are common to all three environments; migration terms will be incorporated and explained in the following habitat subsections. The rate of change of the feeding adult population is expressed as the maturation of females from the pupa stage (n_p) less transition into egg-laying (n_a) and death (d_a). An additional term is included to represent the rate of return from the egg-laying stage to enter an additional oviposition cycle, which is expressed as the fraction of adults returning to complete another oviposition cycle ($\frac{1}{2}$), times the inverse of the length of an oviposition cycle ($\frac{1}{l_v}$), times the number of egg-laying adults (A_2).

$$(6) A' = \frac{n_p}{2}P - (d_a + n_a)A + \frac{1}{2} * \frac{1}{l_v} A_2$$

The rate of change of the egg-laying adult population is expressed as transition into egg-laying (n_a), less death (d_a) and the rate of transition out of egg-laying ($\frac{1}{l_v}$), which is the inverse of the length of an oviposition cycle.

$$(7) A'_2 = n_a A - d_a A_2 - \frac{1}{l_v} A_2$$

A third adult stage is included to represent the population of adult females that have exited the egg-laying stage for the final time. The rate of change of this population is expressed as the exit rate from the final oviposition cycle ($\frac{1}{2} * \frac{1}{l_v}$), less death (d_a).

$$(8) A'_3 = \frac{1}{2} * \frac{1}{l_v} A_2 - d_a A_3$$

Table 1 lists descriptions of the parameters and variables included in these eight equations, along with units and the sources from which they are derived. Temperature-dependent parameters, which include eggs laid per female per day (e_b), larval and pupal maturation and death rates ($n_{Ls}, n_{Lb}, n_p, f_s, f_b, f_p$), and the length of the oviposition cycle (l_v), are listed alongside the equations that determine their values. All other parameters, including egg flooding, hatching, and death rates ($n_{Ed}, n_{Ew}, q_{Ed}, q_{Ew}$), density-dependent larval death rates (q_{Ew}, q_{Ed}),

the rate of adult transition into egg-laying (n_a), and the daily adult death rate (d_a), are listed with constant values.

2.1.1 Outdoor Habitat Modifications

As the first habitat in our model, we consider outdoor environments, which we categorize as non-enclosed, non-temperature-controlled spaces that are exposed to regular weather patterns. Examples of significant outdoor habitats in the U.S. cities of interest include yards and public parks, where flower pots, domestic animal feeding dishes, and other unattended wet or rain-filled containers provide breeding sites for mosquitos (Barrera et al. 2006). *Aedes aegypti* mosquitos in outdoor habitats are assumed to mature according to the eight equations described above, with modifications included only to describe migration in the A and A_2 —adult feeding and egg-laying—stages. Equations (1) through (5) determine changes in the outdoor aquatic population as listed above.

The rate of change of the outdoor feeding adult population is determined as in Equation (6), with three added migration terms. Feeding adults are assumed to migrate into the outdoor habitat from uninhabited enclosed environments in search of humans to bite, leading to growth in the outdoor feeding population. Growth also occurs as a result of feeding adults traveling from indoor to outdoor spaces. Feeding adults can migrate out of the outdoor habitat in search of blood meals in indoor spaces; however, they are assumed not to migrate from outdoor to enclosed habitats, as no human subjects are available to bite in enclosed water tanks. Thus, migration during the outdoor feeding adult stage is expressed as the sum of the rates of migration from enclosed and indoor spaces (m_{eo}, m_{io}), less the outdoor-to-indoor migration rate (m_{oi}).

$$A'_o = \frac{n_p}{2} P_o - (d_a + n_a) A_o + \frac{1}{2} * \frac{1}{l_v} A_{2o} + m_{eo} A_e + m_{io} A_i - m_{oi} A_o$$

The rate of change of the outdoor egg-laying population is determined as in Equation (7), with three added migration terms. As in the feeding stage, both outdoor-to-indoor and indoor-to-outdoor migration are included during laying to represent the movement of vectors between buildings and outdoor environments. The arrival of laying adults from indoor spaces (m_{2io}) leads to growth in the outdoor population, while the rate of departure to indoor environments (m_{2oi}) is subtracted from the equation. Departure from outdoor to enclosed environments (m_{2oe}) is also included, but we assume that no laying adults arrive outdoors from enclosed habitats, as these

habitats are defined as entirely wet spaces and are optimal for oviposition. Migration during the outdoor A_2 stage is expressed as follows.

$$A'_{2o} = n_a A_o - d_a A_{2o} - \frac{1}{l_v} A_{2o} + m_{2io} A_{2i} - m_{2oe} A_{2o} - m_{2oi} A_{2o}$$

There is no longer a need for migration once mosquitos have finished feeding and laying eggs, so the rate of change of the outdoor A_3 population is determined by Equation (8).

2.1.2 Indoor Habitat Modifications

The second habitat category includes indoor environments, which are defined as enclosed, temperature-controlled, manmade spaces, such as homes and buildings, that are not exposed to typical climate variations. The main difference between the indoor and outdoor habitats is that indoor temperature remains at a constant level year-round; similar equations otherwise determine maturation rates within the two environments. Equations (1) to (5) determine changes in the indoor aquatic population as listed above.

The rate of change of the indoor feeding adult population is determined as in Equation (6), with two added migration terms. Because our habitat structure assumes that there are no adjacent indoor and enclosed spaces—that is, a mosquito cannot travel from a house to a water tower without first traveling outside—no term is included to describe migration between indoor and enclosed environments. However, as humans travel frequently between indoor and outdoor environments, feeding mosquitos are assumed to move similarly between the two habitats in search of subjects to bite. The two migration terms describe the rate of indoor feeding population increase as a result of the arrival of mosquitos from outdoors (m_{oi}), and the rate of decrease as a result of departure to outdoor habitats (m_{io}).

$$A'_i = \frac{n_p}{2} P_i - (d_a + n_a) A_i + \frac{1}{2} * \frac{1}{l_v} A_{2i} + m_{oi} A_o - m_{io} A_i$$

The rate of change of the indoor egg-laying population is determined as in Equation (7), with two added migration terms. As fluctuations occur in the indoor and outdoor aquatic habitat areas due to the filling and emptying of manmade containers, the vector must adjust its location to seek optimal oviposition sites. We include migration terms in each direction (m_{2oi} , m_{2io}) to represent the movement of laying adults among indoor and outdoor habitats.

$$A'_{2i} = n_a A_i - d_a A_{2i} - \frac{1}{l_v} A_{2i} + m_{2oi} A_{2o} - m_{2io} A_{2i}$$

Like the outdoor post-egg-laying population, indoor A_3 adults have no need for migration and their population fluctuates as in Equation (8).

2.1.3 Enclosed Habitat Modifications

The final habitat category includes enclosed, water-filled environments such as sewers and water tanks that are sheltered from extreme outdoor temperature variations but not climate-controlled to the extent of indoor habitats. Two unique assumptions defining the enclosed habitat are that it is entirely wet and that it has no human subjects available for biting (Russell et al. 2001). These characteristics alter both the oviposition and migration patterns for adults in enclosed habitats: Eggs are laid exclusively in wet areas, but adults must migrate outdoors to feed before returning for oviposition.

Given that all eggs are laid in wet spaces within enclosed water tanks, Equation (1), which describes the rate of change of the dry egg population, is not relevant to the enclosed habitat. Equation (2) thus describes the rate of change of the total enclosed egg population as listed above. The proportion of eggs laid in aquatic habitat (p_w) is assumed to be 1, and no term is included to represent the dry egg flooding rate.

$$E_{we}' = e_b A_{2e} - n_{Ew} E_{we} - q_{Ew} E_{we}$$

The rates of change of the subsequent enclosed aquatic populations are determined as in Equations (3) to (5).

The rate of change of the enclosed feeding adult population is determined as in Equation (6), with one added migration term. Because it is not possible to feed in an uninhabited enclosed environment, no feeding adults are assumed to migrate into the enclosed habitat. Conversely, all enclosed feeding adults must migrate outdoors to find blood meals. Migration among enclosed feeding adults thus includes only departure to the outdoor habitat (m_{eo}). Furthermore, no maturation term from the enclosed feeding to egg-laying stage is included, as this transition is not possible without first migrating outdoors to feed.

$$A_e' = \frac{n_p}{2} P_e - d_a A_e + \frac{1}{2} * \frac{1}{l_v} A_{2e} - m_{eo} A_e$$

The rate of change of the enclosed egg-laying adult population is determined as in Equation (7), with population growth occurring as a result of migration from the outdoor habitat rather than maturation from the enclosed feeding stage. Fluctuations in this enclosed stage are

determined by the rate of migration from outdoors (m_{2oe}), less death and the rate of transition out of egg-laying.

$$A'_{2e} = m_{2oe}A_{2o} - d_a A_{2e} - \frac{1}{l_v} A_{2e}$$

The rate of change of the enclosed A_3 population is determined as in Equation (8).

2.1.4 Complete System of Habitat-Specific Equations

Including all of the modifications described above, the complete model consists of 23 ordinary differential equations, which include two systems of eight equations for the outdoor and indoor habitats and a system of seven equations for the enclosed habitat. The system of equations by habitat, including both biological and spatial transition terms, is as follows.

Outdoor habitat model:

$$\begin{aligned} E_{do}' &= (1 - p_{wo})e_b A_{2o} - n_{Ed} E_{do} - q_{Ed} E_{do} \\ E_{wo}' &= p_{wo}e_b A_{2o} + n_{Ed} E_{do} - n_{EW} E_{wo} - q_{EW} E_{wo} \\ L_{so}' &= n_{EW} E_{wo} - (f_s + n_{LS})L_{so} - \frac{q_{LS}}{k_o} L_{so}^2 \\ L_{bo}' &= n_{LS} L_{so} - (f_b + n_{Lb})L_{bo} - \frac{q_{Lb}}{k_o} L_{bo}^2 \\ P_o' &= n_{Lb} L_{bo} - (f_p + n_p)P_o \\ A_o' &= \frac{n_p}{2} P_o - (d_a + n_a)A_o + \frac{1}{2} * \frac{1}{l_v} A_{2o} + m_{eo} A_e + m_{io} A_i - m_{oi} A_o \\ A_{2o}' &= n_a A_o - d_a A_{2o} - \frac{1}{l_v} A_{2o} + m_{2io} A_{2i} - m_{2oe} A_{2o} - m_{2oi} A_{2o} \\ A_{3o}' &= \frac{1}{2} * \frac{1}{l_v} A_{2o} - d_a A_{3o} \end{aligned}$$

Indoor habitat model:

$$\begin{aligned} E_{di}' &= (1 - p_{wi})e_b A_{2i} - n_{Ed} E_{di} - q_{Ed} E_{di} \\ E_{wi}' &= p_{wi}e_b A_{2i} + n_{Ed} E_{di} - n_{EW} E_{wi} - q_{EW} E_{wi} \\ L_{si}' &= n_{EW} E_{wi} - (f_s + n_{LS})L_{si} - \frac{q_{LS}}{k_i} L_{si}^2 \\ L_{bi}' &= n_{LS} L_{si} - (f_b + n_{Lb})L_{bi} - \frac{q_{Lb}}{k_i} L_{bi}^2 \\ P_i' &= n_{Lb} L_{bi} - (f_p + n_p)P_i \\ A_i' &= \frac{n_p}{2} P_i - (d_a + n_a)A_i + \frac{1}{2} * \frac{1}{l_v} A_{2i} + m_{oi} A_o - m_{io} A_i \\ A_{2i}' &= n_a A_i - d_a A_{2i} - \frac{1}{l_v} A_{2i} + m_{2oi} A_{2o} - m_{2io} A_{2i} \\ A_{3i}' &= \frac{1}{2} * \frac{1}{l_v} A_{2i} - d_a A_{3i} \end{aligned}$$

Enclosed habitat model:

$$\begin{aligned}E_{we}' &= e_b A_{2e} - n_{EW} E_{we} - q_{EW} E_{we} \\L_{se}' &= n_{EW} E_{we} - (f_s + n_{LS}) L_{se} - \frac{q_{LS}}{k_e} L_{se}^2 \\L_{be}' &= n_{LS} L_{se} - (f_b + n_{Lb}) L_{be} - \frac{q_{Lb}}{k_e} L_{be}^2 \\P_e' &= n_{Lb} L_{be} - (f_p + n_p) P_e \\A_e' &= \frac{n_p}{2} P_e - d_a A_e + \frac{1}{2} * \frac{1}{l_v} A_{2e} - m_{eo} A_e \\A_{2e}' &= m_{2oe} A_{2o} - d_a A_{2e} - \frac{1}{l_v} A_{2e} \\A_{3e}' &= \frac{1}{2} * \frac{1}{l_v} A_{2e} - d_a A_{3e}\end{aligned}$$

2.2 El Paso Climate

Several of the maturation and death parameters in the above model depend upon temperature and the available habitat area. In this section, we establish initial climate models for the three habitats in the example city of El Paso, which underpin our subsequent derivation of temperature-dependent parameters. Similar climate models are defined for the other five cities of interest in the subsequent numerical simulations.

2.2.1 Outdoor Temperature

To represent annual outdoor weather patterns, we derive a model based on daily average temperature data from El Paso (U.S. Climate Data). Temperatures range from an annual low of 6°C in early January to highs of over 28°C in July, making the viability of mosquito survival highly variable. We find a best-fit model for two years of climate data by fitting a function to two iterations of the annual daily mean temperature, as shown in Figure 2. The following Fourier equation reflects seasonal temperature fluctuations in El Paso, where t represents the number of days since January 1st of the first year.

$$(9) T_{outdoor} = 18.08 - 10.67 \cos(.01713t) - 2.302 \sin (.01713t)$$

2.2.2 Indoor Temperature

Because indoor spaces are climate-controlled by definition, we assume that the indoor habitat remains at a constant temperature year-round. We choose an average indoor temperature of 21°C, which falls within the typical range for climate-controlled American households. Temperatures in the indoor habitat are defined by the following constant function.

$$(10) T_{indoor} = 21$$

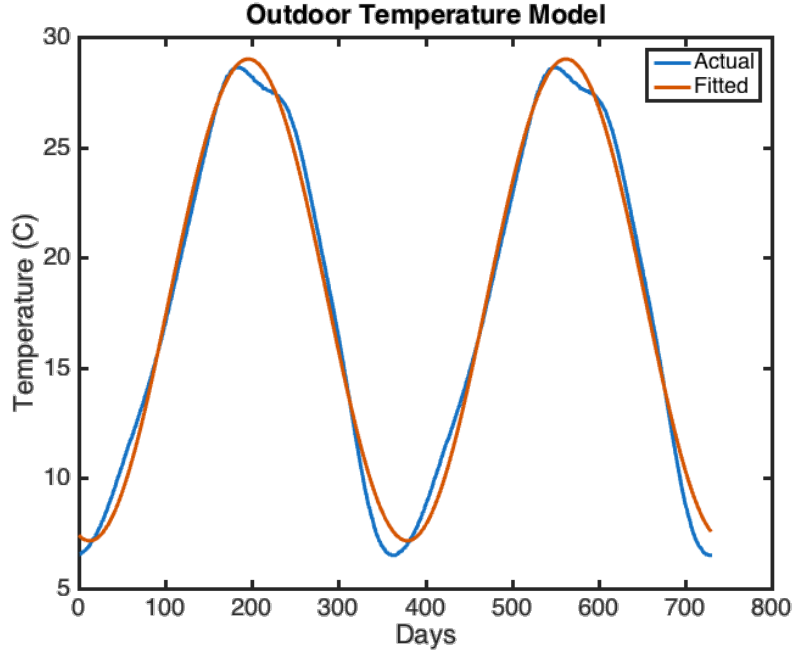


Figure 2. Outdoor temperature model for El Paso, TX. The blue (Actual) line shows two iterations of one year of reported average daily temperatures. The orange (Fitted) line shows the best-fit Fourier equation to predict temperature over the same period. This function is specified in Equation (9) and subsequently used as the outdoor temperature input for the model in El Paso.

2.2.3 Enclosed Temperature

While data on the annual daily temperature of enclosed water tanks and sewers is scarce, we use the reported relationship between underground and surface temperatures as a proxy for the insulating effect of enclosed habitats. In a study of underground wine storage areas, Tinti et al. report an external temperature amplitude of 15.5°C and an underground temperature amplitude of 7.6°C , implying that the ratio of the size of underground to above-ground fluctuations is .49 (Tinti et al. 2015). In addition to scaling the amplitude of the outdoor Fourier function by this value, we introduce a lag of two weeks between outdoor and enclosed temperatures. This timing modification is based upon the assumption that insulated spaces tend to retain heat and cold for longer periods than exposed environments, as well as Naylor’s finding that underground soil reached its annual peak temperature about 14 days after the soil surface in Indiana (Naylor 2017). The resulting function determines the temperature of the enclosed habitat.

$$(11) T_{enclosed} = 18.08 - .49(10.67 \cos(.01713(t - 14)) + 2.302 \sin(.01713(t - 14)))$$

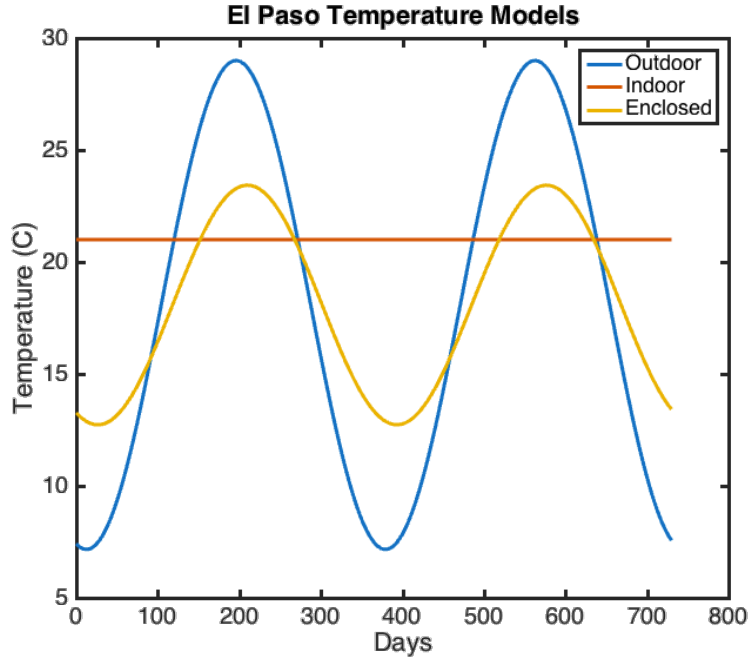


Figure 3. A comparison of outdoor, indoor, and enclosed temperature models for El Paso, TX. The blue (Outdoor) curve shows the best-fit function specified in Equation (9), the orange (Indoor) line shows constant temperature in climate-controlled spaces, and the yellow (Enclosed) curve shows the modifications specified in Equation (11) that represent a smaller amplitude and time lag for enclosed temperatures.

2.3 Lifecycle Parameters

The establishment of equations describing temperature fluctuations in three habitat types allows us to calculate the complete set of maturation and death parameters for the system of differential equations described above. In this section, we discuss the derivation of either a constant value or a temperature-dependent function for each population parameter in the model.

2.3.1 Egg Production Rates

Egg production is determined by the proportion of eggs that are laid in wet habitats (p_w), the number of egg-laying adult females (A_2), and the number of eggs produced per female per day (e_b). In a study of oviposition preferences, Edman et al. found that only 5.8% of initially gravid *Aedes aegypti* mosquitoes were recaptured in their original locations when left to lay in entirely dry environments (Edman et al. 1998). Based on this finding, we assume a high rate of departure from each habitat in the absence of wet laying area, which we subsequently incorporate into our migration rates.

For the adults remaining in the indoor and outdoor habitats during oviposition, we take the proportion laying in aquatic habitat to be very close to one unless there is no aquatic habitat available. Wet laying rates are accordingly set to $p_{wo} = \frac{k_o}{.1+k_o}$ and $p_{wi} = \frac{k_i}{.1+k_i}$, where k_o and k_i are the areas of aquatic outdoor and indoor habitat, respectively. The value of .1 in the denominator represents the half saturation constant, or the area of existing aquatic habitat at which half of all eggs will be laid in wet habitat and half in dry habitat. We select a relatively small constant to signify that the majority of eggs will be laid in wet places unless there is very little aquatic habitat available. However, the half saturation constant has yet to be fully explored and could take on an even smaller value in future research to reflect a stronger preference for aquatic laying habitat. In enclosed areas, we assume a 100% wet laying proportion based on the definition of these habitats as water-filled spaces.

Costa et al. report the mean number of eggs laid daily per adult female under two humidity conditions at each of three temperatures (Costa et al. 2010). We average these results at 25°C, 30°C, and 35°C and set the number of eggs laid daily to zero at 10°C and 40°C based on Yang's observation that oviposition did not occur at or beyond these temperatures (Yang 2009). We use these data to find a best-fit Gaussian function describing the number of eggs laid per female per day by temperature, which is used to derive e_b for each temperature and habitat. Values of this function are shown by temperature in Figure 5A.

$$(12) e_b = 78.86e^{-\left(\frac{T-29.21}{8.041}\right)^2}$$

We determine the egg production rate in each habitat by multiplying p_w and e_b by the population of adult egg-laying females (A_2), which varies over time.

2.3.2 Egg Flooding and Hatching Rates

Oviposition occurs in either a wet or a dry environment according to the proportion of adult females laying in wet habitats. While eggs can remain viable for several months under dry conditions, they must become submerged via a flooding event and enter the wet state before hatching (Focks et al. 1993). We consider human activity to be the main source of flooding, given that our model assumes breeding to take place in primarily manmade containers. In the outdoor habitat, flooding occurs through lawn watering, sprinklers, and the filling of other outdoor dishes and containers. Based on assumptions about general human behavior, we presume that about half of these containers are filled through one of the aforementioned events each week,

resulting in a daily outdoor flooding rate (n_{Ed}) of .071. Indoors, similar activities lead to egg submergence: We consider the filling of animal dishes, flower pots, and other containers to be the main flooding events. Assuming that humans' indoor container filling behaviors do not differ significantly from outdoor ones, we apply the same flooding rate to the indoor habitat. There is no enclosed habitat flooding rate, as all eggs in this habitat are initially laid in aquatic areas.

For eggs laid in wet environments, and for originally dry eggs that have become submerged, transition out of the egg stage is determined by the hatching rate (n_{Ew}). Focks et al. report a daily mean hatching rate of 59.6% among wet eggs when submerged in water above 22°C; however, they acknowledge that this threshold may be too high based on Christophers' observation of successful hatching between 13°C and 20°C (Focks et al. 1993; Christophers 1960). We therefore assume that a uniform daily hatching rate of .596 determines transition from the wet egg to small larva stage.

2.3.3 Egg Death Rates

Faull and Williams report the mean survival time of *Aedes aegypti* eggs at varying levels of warmth and dryness to show the ongoing survival and viability of eggs laid in dry locations. On average, the eggs that the researchers observed could survive 187.4 days under dry conditions and 229.3 days under wet conditions (Faull and Williams 2015). To represent the failure of unhatched eggs to remain viable beyond these time periods, we invert the mean survival times and derive death rates of .0053 and .0044 for dry and wet eggs, respectively. These are the values given for q_{Ed} and q_{Ew} in the model.

2.3.4 Maturation Rates for Larvae and Pupae

In the larval and pupal stages, maturation parameters are temperature-dependent. Tun-Lin studied maturation times and survival rates at five different temperatures, ranging from 15°C to 35°C, in Queensland, Australia, and found that the time to maturation decreased consistently as temperatures rose within this range (Tun-Lin et al. 2000).

While Tun-Lin recorded maturation times at five stages of development—larval groups L₁ through L₄ and P—we modify this structure by combining L₁ with L₂ and L₃ with L₄ to derive temperature-dependent maturation parameters for our two larval categories, small and big larvae. Doing so makes it possible for our study to incorporate information from other reports, whether they consider larval development to include two or four stages. Larval maturation times M_i are

measured as $M_{Ls} = M_{L1} + M_{L2}$ and $M_{Lb} = M_{L3} + M_{L4}$. We invert these total maturation times to find mean maturation rates at each temperature for small larvae, big larvae, and pupae. We plot maturation rate as a function of temperature, $R(T)$, at each stage and fit a Gaussian curve of the following form to describe temperature-dependent maturation rates:

$$(13) R(T) = ae^{(-\frac{T-b}{c})^2}$$

Parameter values for the best-fit equation at each stage are recorded in Table 1 and shown in Figures 5B – 5D. Within the model, these three best-fit equations determine temperature-dependent maturation rates for small larvae (n_{Ls}), big larvae (n_{Lb}), and pupae (n_P) as weather conditions fluctuate.

2.3.5 Temperature-Dependent Death Rates for Larvae and Pupae

Tun-Lin's observations of survival rates and maturation times at each of five temperatures also facilitate the calculation of density-independent death rates for larvae and pupae. At each temperature, Tun-Lin records the probability of survival to adulthood, $S(T)$, and the total maturation time in days, $X(T)$. We derive D , a density-independent death rate relating temperature, emergence time, and survival rate, as follows, where y is the percentage of the population surviving at a given time:

$$\begin{aligned} y' &= -Dy \\ y &= ce^{-DX(T)} \\ y(0) &= 100 \rightarrow y = 100e^{-DX(T)} \\ S(T) &= e^{-DX(T)} \\ \ln(S(T)) &= -DX(T) \\ D &= -\frac{\ln(S(T))}{X(T)} \end{aligned}$$

We assume that temperature-dependent death rates are the same for small and big larvae and pupae, and fit a polynomial to the D value calculated from Tun-Lin's results at each temperature. The resulting equation determines density-independent death rates— f_s , f_b , and f_P —as a function of temperature, T .

$$(14) D(T) = 5.311E(-6)T^4 - .0005T^3 + .0195T^2 - .316T + 1.901$$

Figure 4 affirms that the values of D as determined by this polynomial remain greater than zero both within and beyond the temperature range included in Tun-Lin’s study. We are able to proceed using this best-fit polynomial without concern for producing negative death rate values.

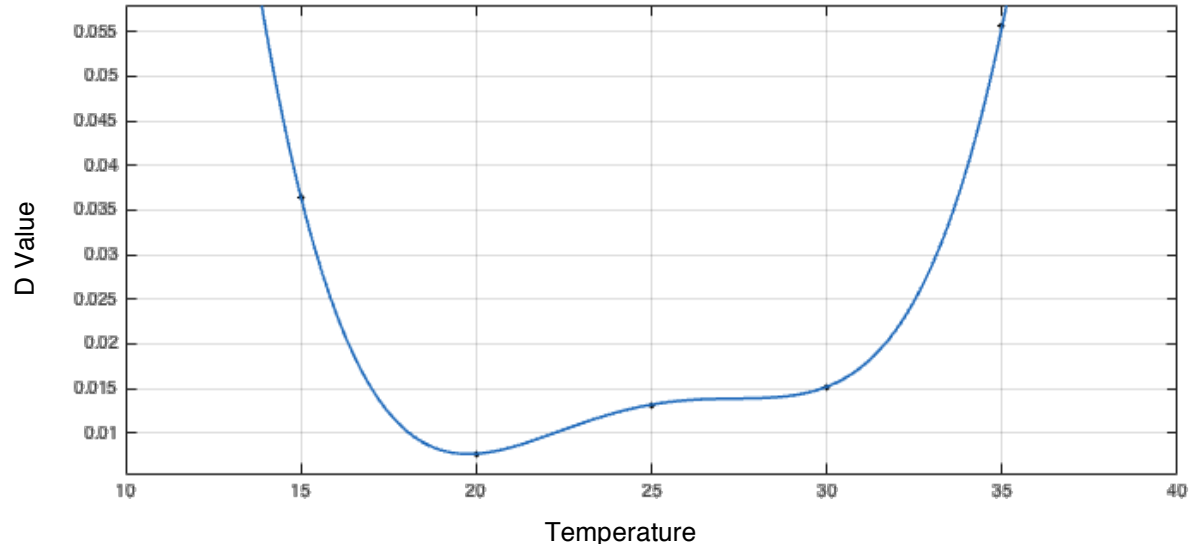


Figure 4. Curve fitting session to determine the best-fit value of D by temperature from five observed values. The fourth degree polynomial is uniformly positive on the interval from 10°C to 40°C , and its value continues to increase on either end of this range.

2.3.6 Density-Dependent Death Rates for Larvae

In addition to a temperature-dependent death rate, we include density-dependent death rates in the larval stages to account for the effects of crowding and to reproduce instar ratios observed in the field (Wallace et al. 2017). Southwood et al. observed mean daily adult emergence rates during a study in Thailand, as well as counts of eggs, larvae, and pupae appearing in containers such as water jars and flower pot plates. Water jars were the primary breeding areas for mosquitos, with an average of 54.84 adults emerging daily from 100 jars (Southwood et al. 1972). We take the surface area estimate of 1 m^2 for the average water jar in Thailand to calculate a daily mean emergence rate of .5484 adults per m^2 of water available for breeding (Visvanathan et al. 2015). This rate corresponds to $n_p P$ in Equation (6) of the model.

We solve the remaining equations at equilibrium at a constant temperature of 21°C , which is our defined indoor temperature and falls within the range of outdoor temperatures in El Paso. Southwood’s emergence rate provides a constant value for P at this temperature.

$$P = \frac{.5484}{n_p}$$

We rearrange Equation (5) at equilibrium to derive the number of big larvae.

$$L_b = \frac{(f_p + n_p) P}{n_{Lb}}$$

We substitute the L_b value into Equation (4) and again rearrange the terms at equilibrium, resulting in an expression for the value of q_{Lb} as a function of the ratio of small to big larvae.

$$q_{Lb} = \frac{k}{L_b} \left(n_{Ls} \left(\frac{L_s}{L_b} \right) - (f_b + n_{Lb}) \right)$$

Southwood et al. report larval counts over the course of one year in water jars, and we average these values to derive a ratio of small to big larvae of 389/190. Substituting the known constant values for all other parameters in the equation results in a density-dependent death rate of .074 for big larvae.

Finally, we perform the same substitutions for Equation (3) at equilibrium to derive the value of q_{Ls} based on the ratio of wet eggs to small larvae.

$$q_{Ls} = \frac{k}{L_s} \left(n_{Ew} \left(\frac{E_w}{L_s} \right) - (f_s + n_{Ls}) \right)$$

We solve with the reported wet egg to small larvae count ratio of 2366/389 to derive a density-dependent death rate of .060 for small larvae. With these values for q_{Ls} and q_{Lb} , the model reproduces the instar ratios from Southwood's field study when the system is solved at equilibrium.

2.3.7 Adult Transition and Death Rates

The pupal maturation rate (n_p) determines the rate of initial entry into the feeding adult stage. We divide this value in half to include only adult females, the only group that feeds and reproduces, assuming a 1:1 sex ratio (Sheppard et al. 1969). In addition to maturing from the aquatic stages into a first feeding cycle, vectors re-enter the feeding adult stage between reproductive periods. Judson observed that oviposition took place twice on average among adults; half of the females exiting the egg-laying stage therefore return to the feeding stage to begin another cycle (Judson 1967).

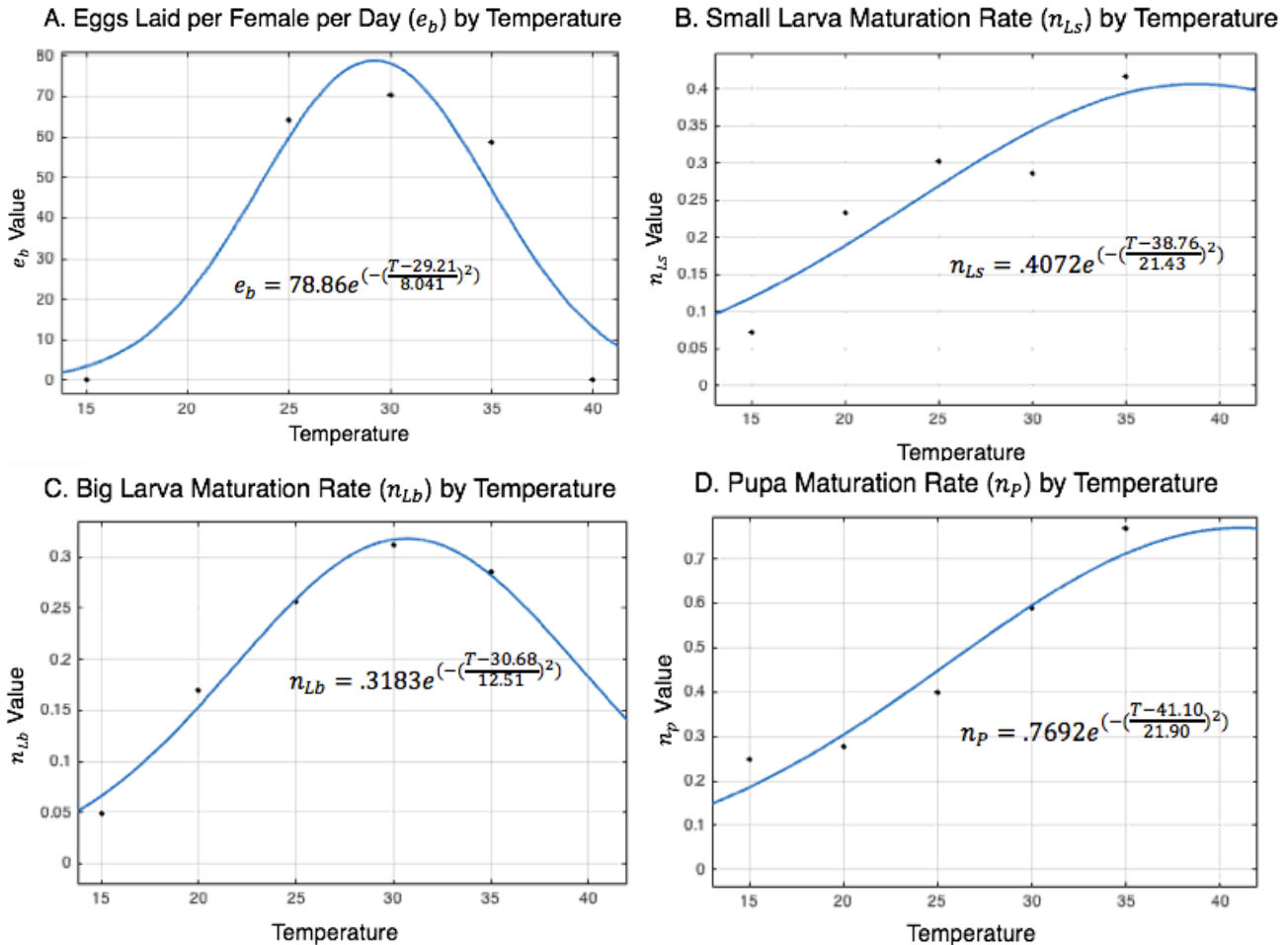
The feeding population decreases in part as a result of transition into the egg-laying stage. Based on Costa's observation that mosquitos did not lay eggs within the first three days of reaching adulthood under any weather conditions, we take the rate of maturation out of the

feeding stage (n_a) to be 1/3 (Costa et al. 2010). We also include a daily adult death rate (d_a) of .11, corresponding to a mean daily adult survival rate of 89% (McDonald 1977).

Adults transition into the egg-laying stage from the feeding stage, and the egg-laying population decreases as a result of the end of each oviposition cycle and death. The length of an oviposition cycle is temperature-dependent, with particularly warm or cold conditions inhibiting adults' ability to survive and lay eggs for more than a few days (Costa et al. 2010). We fit the following Gaussian function to Costa's oviposition cycle data to describe the length of the egg-laying period by temperature. Values are shown in Figure 5F.

$$(15) l_v = 4.727e^{-\left(\frac{T-26.16}{7.574}\right)^2}$$

At each temperature, the rate at which adults exit the egg-laying stage—either to begin another feeding period or to complete the final oviposition cycle—is taken as the inverse of this value ($\frac{1}{l_v}$). The death rates of egg-laying and post-egg-laying adults take on the same constant value as the death rate of feeding adults (d_a).



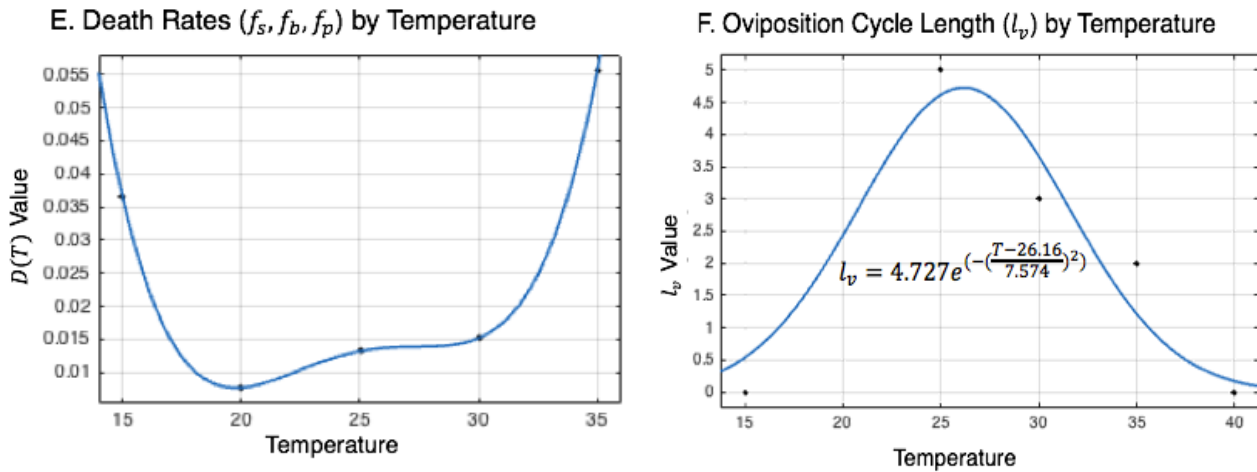


Figure 5. Curve fitting sessions to determine the best-fit values for temperature-dependent equation parameters. The big larva maturation rate, oviposition cycle length, and eggs laid daily per female peak in the middle of the temperature range, between 25°C and 30°C. The remaining two maturation rates peak at warmer temperatures of around 35°C. Death rates are lowest between 20°C and 30°C, indicating that moderate temperatures are most conducive to daily survival.

2.3.8 Migration Rates

Because of the limited availability of data describing mosquito migration patterns among the habitat types we consider, we estimate migration rates based on the vector’s needs in each stage of the gonotrophic cycle. The rates of migration among the three habitats in the feeding stage are determined by the availability of humans to bite. We assume that all feeding mosquitoes in the enclosed habitat migrate to the outdoor habitat ($m_{eo} = 1$), as there is otherwise no way for this subpopulation to feed. We estimate migration rates between the indoor and outdoor habitats based upon the proportion of the time that humans spend in each environment. Given that the average person spends about two hours outdoors per day, and under the simplifying assumption that this time is evenly distributed, we assume that 8.3% of humans are outdoors and 91.7% are indoors at any given time (Diffey 2011). We divide these values by three days, the average length of the feeding period, to derive daily outdoor-to-indoor and indoor-to-outdoor feeding migration rates (m_{oi}, m_{io}).

During the egg-laying stage, we treat migration among habitats as a function of the available wet oviposition area in each environment. The constants k_o , k_i , and k_e represent the areas of outdoor, indoor, and enclosed aquatic habitat, respectively, resulting in a total wet laying area of $k_{tot} = k_o + k_i + k_e$. We assume based on Edman’s study that $\alpha = 94.2\%$ of adults leave

each habitat during the oviposition period in the complete absence of wet laying area (Edman et al. 1998). For indoor to outdoor migration, we multiply this value by $(\frac{k_o}{k_o+k_i})$, the proportion of the combined indoor and outdoor environments made up by the outdoor habitat. Doing so results in an indoor-to-outdoor migration rate of 94.2% in the complete absence of wet indoor laying area, and a 0% indoor-to-outdoor migration rate in the complete absence of wet outdoor laying area. We divide this rate by l_v , the length of the oviposition period, to represent daily migration.

The remaining two oviposition migration rates describe migration from the outdoor habitat to indoor and enclosed areas. For each of these rates, we first multiply α by $(1 - \frac{k_o}{k_{tot}})$, resulting in a rate that is inversely related to the proportion of the total wet laying area that the outdoor aquatic habitat comprises. We additionally multiply the outdoor-to-indoor and outdoor-to-enclosed rates by $(\frac{k_i}{k_i+k_e})$ and $(\frac{k_e}{k_i+k_e})$, respectively, so that the rate of migration to each habitat depends upon its relative availability. In the absence of either indoor or enclosed oviposition habitat, the laying adults leaving the outdoor habitat will thus reach the destination in which aquatic laying area is present.

Table 1. Description of parameters and variables

Variables

Symbol	Value	Units	Description	Source
E_d	Variable	Number	Dry egg population	-
E_w	Variable	Number	Wet egg population	-
L_s	Variable	Number	Small larva population	-
L_b	Variable	Number	Big larva population	-
P	Variable	Number	Pupa population	-
A	Variable	Number	Feeding adult population	-
A_2	Variable	Number	Laying adult population	-
A_3	Variable	Number	Post-laying adult population	-

Constant parameters

Symbol	Value	Units	Description	Source
α	.9420	-	Proportion of adults dispersing in the absence of wet habitat	Edman 1998
n_{Ed}	.0710	Days ⁻¹	Egg flooding rate	-

n_{Ew}	.5960	Days ⁻¹	Egg hatching rate	Focks 1993
q_{Ed}	.0053	Days ⁻¹	Dry egg death rate	Faull 2015
q_{Ew}	.0044	Days ⁻¹	Wet egg death rate	Faull 2015
q_{Ls}	.0600	Days ⁻¹	Density-dependent small larva death rate	Southwood 1972
q_{Lb}	.0740	Days ⁻¹	Density-dependent big larva death rate	Southwood 1972
n_a	1/3	Days ⁻¹	Rate of adult transition to egg-laying	Costa 2010
d_a	.1100	Days ⁻¹	Daily adult death rate	McDonald 1977

Temperature-Dependent Parameters

Symbol	Function	Description	Source
e_b	$78.86e^{-(\frac{T-29.21}{8.041})^2}$	Eggs laid per female per day	Costa 2010
n_{Ls}	$.4072e^{-(\frac{T-38.76}{21.43})^2}$	Small larva maturation rate	Tun-Lin 2000
n_{Lb}	$.3183e^{-(\frac{T-30.68}{12.51})^2}$	Big larva maturation rate	Tun-Lin 2000
n_p	$.7692e^{-(\frac{T-41.10}{21.90})^2}$	Pupa maturation rate	Tun-Lin 2000
f_s, f_b, f_p	$5.311E(-6)T^4 - .0005T^3 + .0195T^2 - .316T + 1.901$	Density-independent death rates for larvae and pupae	Tun-Lin 2000
l_v	$4.727e^{-(\frac{T-26.16}{7.574})^2}$	Length of oviposition cycle	Costa 2010

Habitat and Migration Parameters

Symbol	Value	Units	Description	Source
k_o	Variable	m ²	Outdoor aquatic habitat area	-
k_i	Variable	m ²	Indoor aquatic habitat area	-
k_e	Variable	m ²	Enclosed aquatic habitat area	-
p_{wo}	$\frac{k_o}{.1 + k_o}$	-	Proportion eggs laid in wet habitat, outdoor	-
p_{wi}	$\frac{k_i}{.1 + k_i}$	-	Proportion eggs laid in wet habitat, indoor	-
p_{we}	1	-	Proportion eggs laid in wet habitat, enclosed	-

m_{oi}	$.917/3$	Days ⁻¹	Outdoor-to-indoor daily feeding migration rate	-
m_{io}	$.083/3$	Days ⁻¹	Indoor-to-outdoor daily feeding migration rate	-
m_{eo}	$1/3$	Days ⁻¹	Enclosed-to-outdoor daily feeding migration rate	-
m_{2io}	$\alpha \left(\frac{k_o}{k_o + k_i} \right) \frac{1}{l_v}$	Days ⁻¹	Indoor-to-outdoor daily laying migration rate	-
m_{2oi}	$\alpha \left(1 - \frac{k_o}{k_{tot}} \right) \left(\frac{k_i}{k_i + k_e} \right) \frac{1}{l_v}$	Days ⁻¹	Outdoor-to-indoor daily laying migration rate	-
m_{2oe}	$\alpha \left(1 - \frac{k_o}{k_{tot}} \right) \left(\frac{k_e}{k_i + k_e} \right) \frac{1}{l_v}$	Days ⁻¹	Outdoor-to-enclosed daily laying migration rate	-

3. Model Analysis and Equilibrium Viability

While seasonal temperature fluctuations and migration patterns cause ongoing changes to the vector population in all three habitats, it is possible for the population to reach equilibrium under certain constant temperature conditions. To consider this possibility, we first simplify the system of differential equations to the following structure, which represents a single habitat with constant temperature. We set each differential equation equal to zero to consider a situation in which there are no population changes in any of the eight life stages.

$$0 = (1 - p_w)e_b A_2 - (n_{Ed} + q_{Ed})E_d$$

$$0 = p_w e_b A_2 + n_{Ed} E_d - (n_{Ew} + q_{Ew})E_w$$

$$0 = n_{Ew} E_w - (f_s + n_{Ls})L_s - \frac{q_{Ls}}{k} L_s^2$$

$$0 = n_{Ls} L_s - (f_b + n_{Lb})L_b - \frac{q_{Lb}}{k} L_b^2$$

$$0 = n_{Lb} L_b - (f_p + n_p)P$$

$$0 = \frac{n_p}{2} P - (d_a + n_a)A + \frac{1}{2l_v} A_2$$

$$0 = n_a A - (d_a + \frac{1}{l_v})A_2$$

$$0 = \frac{1}{2l_v} A_2 - d_a A_3$$

By substituting values among these equations to express each in terms of A_2 down to the dry egg stage, we obtain a fourth-degree polynomial describing the size of the egg-laying adult population at equilibrium:

$$(16) \quad 0 = C_1 * (A_2)^4 + C_2 * (A_2)^3 + C_3 * (A_2)^2 + C_4 * A_2$$

where

$$C_1 = -\frac{(n_{ed} + q_{ed})(n_{ew} + q_{ew})q_{ls}}{kn_{ed}n_{ew}} \left(\frac{q_{lb}}{kn_{ls}}\right)^2 \left[\frac{2(f_p + n_p)}{n_{lb}n_p} \left(d_a \left(\frac{d_a}{n_a} + 1 \right) + \frac{1}{l_v} \left(\frac{d_a}{n_a} + \frac{1}{2} \right) \right) \right]^4$$

$$C_2 = -\frac{2(n_{ed} + q_{ed})(n_{ew} + q_{ew})q_{ls}(f_b + n_{lb})q_{lb}}{k^2 n_{ed} n_{ew} n_{ls}^2} \left[\frac{2(f_p + n_p)}{n_{lb}n_p} \left(d_a \left(\frac{d_a}{n_a} + 1 \right) + \frac{1}{l_v} \left(\frac{d_a}{n_a} + \frac{1}{2} \right) \right) \right]^3$$

$$\begin{aligned}
C_3 = & -\frac{(n_{ed} + q_{ed})(n_{ew} + q_{ew})(f_s + n_{ls})q_{lb}}{k * n_{ed}n_{ew}n_{ls}} \left(\frac{2(f_p + n_p)}{n_{lb}n_p} \left(d_a \left(\frac{d_a}{n_a} + 1 \right) + \frac{1}{l_v} \left(\frac{d_a}{n_a} + \frac{1}{2} \right) \right) \right)^2 \\
& - \frac{(n_{ed} + q_{ed})(n_{ew} + q_{ew})q_{ls}}{kn_{ed}n_{ew}} \left[\frac{2(f_b + n_{lb})(f_p + n_p)}{n_{ls}n_{lb}n_p} \left(d_a \left(\frac{d_a}{n_a} + 1 \right) + \frac{1}{l_v} \left(\frac{d_a}{n_a} + \frac{1}{2} \right) \right) \right]^2 \\
C_4 = & \left((1 - p_w)e_b + p_w e_b + p_w e_b \left(\frac{q_{ed}}{n_{ed}} \right) \right) \\
& - \left[\frac{2(n_{ed} + q_{ed})(n_{ew} + q_{ew})(f_{ls} + n_{ls})(f_b + n_{lb})(f_p + n_p)}{n_{ed}n_{ew}n_{ls}n_{lb}n_p} \left(d_a \left(\frac{d_a}{n_a} + 1 \right) \right. \right. \\
& \left. \left. + \frac{1}{l_v} \left(\frac{d_a}{n_a} + \frac{1}{2} \right) \right) \right]
\end{aligned}$$

This polynomial allows us to determine the range of temperatures at which it is possible for the population to reach equilibrium. Descartes' Rule of Signs states that the number of positive roots of a polynomial ordered by decreasing power is either equal to the number of sign changes among its coefficients, or less than this number by an even value. In the above polynomial, the coefficients C_1 , C_2 , and C_3 are negative regardless of temperature, as all are negative products of uniformly positive parameters. However, the coefficient C_4 includes two terms with opposite signs, and is positive if the first term has a larger value than the second. When this fourth coefficient is positive, there is one sign change and the Rule of Signs states that the polynomial has one positive root. This value is the size of the egg-laying adult population, and its existence affirms the viability of equilibrium.

The parameters comprising C_4 offer a biological interpretation of the necessary conditions for equilibrium viability. The first term is an egg production rate, expressed as the sum of the number of wet and dry eggs laid per adult per day and the ratio of the dry egg death to flooding rates. The second is a ratio of the products of the rates of exit, via maturation and death, to the rates of entry, via maturation, for each stage. A large value for this term indicates that death rates far exceed maturation rates, leading to population decline. The negative C_4 value associated with a lack of equilibrium viability affirms that the rate of departure from all population stages exceeds the rate of egg production. Conversely, equilibrium becomes viable when enough eggs are produced daily to compensate for the rate of death or maturation out of each of the subsequent life stages.

Using the temperature-dependent formulas stated in Section 2 for each parameter, we solve for the zeroes that result when the fourth coefficient in Equation (16) is evaluated as a function of temperature. Figure 6 shows the sign of this coefficient and the points where it changes over a temperature range of 15°C to 40°C. We find that the coefficient changes sign at 16.16°C and 38.32°C, indicating that the population cannot reach equilibrium, even under constant temperature conditions, when the temperature is outside of this range.

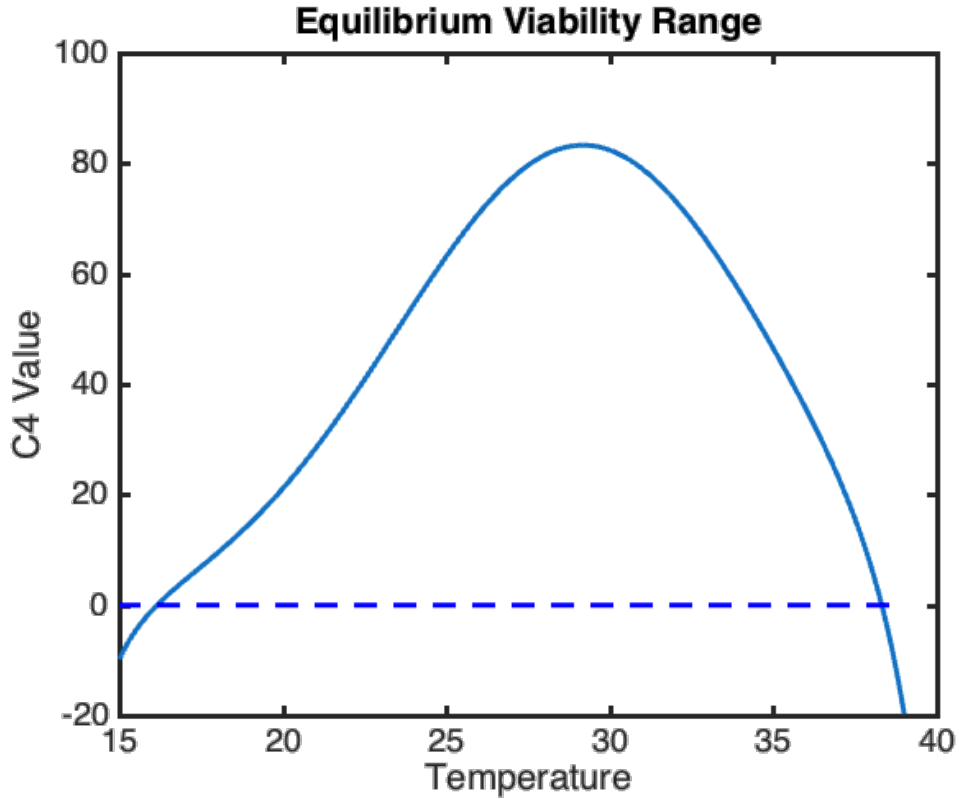


Figure 6. Polynomial coefficient values by temperature. The solid line shows the value of the fourth coefficient in Equation (16) by temperature from 15°C to 40°C, while the dashed line shows the temperature values at which the coefficient passes zero. The graph affirms that the coefficient C_4 changes sign at 16.16°C and 38.32°C.

While the populations in all eight life stages reach constant levels at any temperature within the range shown in Figure 6, the size of the equilibrium population varies by temperature throughout this range. We use MatLab’s ode45 solver to determine the size of the total daily adult population, $A_1 + A_2 + A_3$, that is present given constant temperature conditions at each level from 17°C to 38°C. This value is close to zero on the low end of the temperature spectrum, and it increases non-linearly until reaching a maximum at 30°C, where 28.56 total adults are

present daily per square meter of aquatic habitat. Beyond 30°C, the equilibrium adult population level falls rapidly before again becoming non-existent at the warmest temperatures.

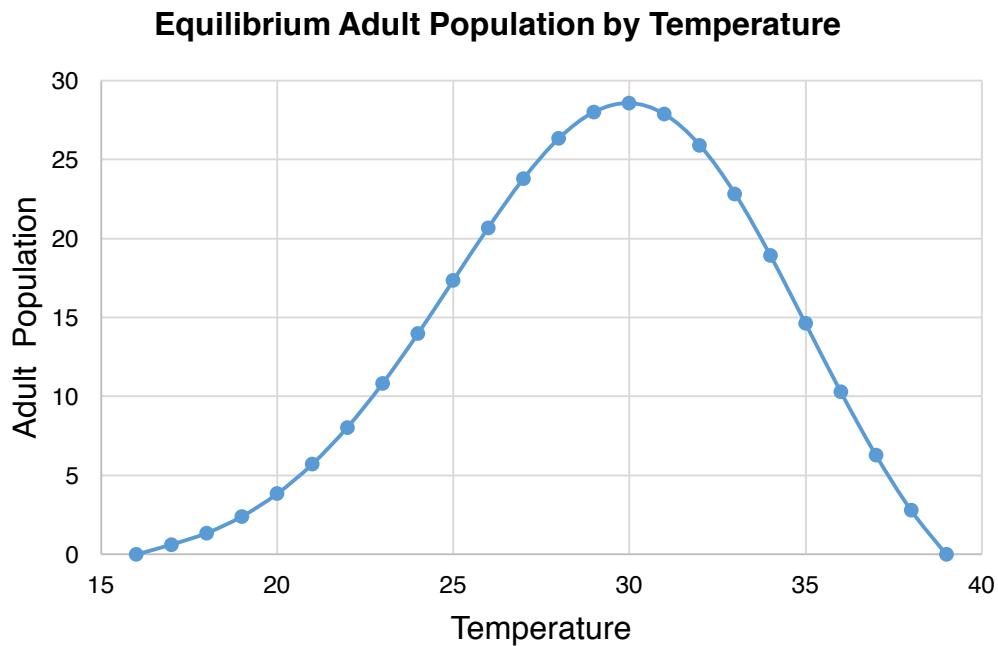


Figure 7. Equilibrium adult population by temperature. At each temperature within the range of equilibrium viability, we solve for the adult population with constant temperature over an adequate period to reach equilibrium. We use the MatLab plotting tool to determine each resulting constant adult population and plot these values as a function of temperature.

In addition to affirming the necessary biological factors for the population to reach equilibrium, the above equations suggest that certain habitat conditions are more conducive than others to vector survival. In outdoor environments with strong temperature fluctuations, an annual disappearance of the adult population is expected when temperatures rise above or fall below the bounds listed above. The equilibrium range suggests that *Aedes aegypti* adults maintain the highest chance of year-round survival in tropical regions where temperatures typically remain between 16°C and 38°C. For indoor environments, the viability findings suggest that while the vector will survive year-round in buildings maintained at the assumed level of 21°C, these conditions do not foster the maximum level of total adult emergence. These interpretations of the equilibrium range facilitate our analysis of habitat viability in the subsequent numerical simulations.

4. Methods

Although the lack of *Aedes aegypti* population data from the field prevents us from validating predicted population levels against actual vector counts, the model and its equilibrium viability range allow us to examine several questions regarding the growth and survival of the vector population. In this section, we provide an overview of the methods used to investigate each question we pose regarding the vector's response to varying habitat types and model parameters. In the first simulation, we model habitat balance, both examining the extreme theoretical cases of homogenous outdoor, indoor, and enclosed habitat and evaluating the optimal balance between these spaces in El Paso. In the second, we define the differences in adult population levels among regions of the United States given varying climates and egg flooding rates. Our third set of simulations investigates the effect of re-introducing indoor habitat to regions in which the vector can survive year-round organically and regions in which it cannot. All simulations are conducted by evaluating the established system of 23 differential equations using MatLab's ode45 solver.

4.1 Modeling Habitat Variation

Given that migration and aquatic survival rates depend upon habitat area, with some habitats offering more optimal temperature and wetness conditions than others, the distribution of habitat types plays a central role in vector emergence (Chan et al. 1971). In our initial simulations, we investigate the effect on the vector population of varying the available proportions of indoor, outdoor, and enclosed aquatic habitat given a fixed total habitat area. We simulate population dynamics resulting from scenarios in which the aquatic habitat is exclusively outdoors, exclusively indoors, and exclusively enclosed. We then approximate the optimal balance among habitat types by investigating the peak and minimum population levels and total annual adult counts that result over a range of habitat ratios in El Paso. We maintain all model parameters as listed above and determine temperature-dependent values using the initial climate model specified in Equations (9) to (11).

The homogenous habitat results, which we display in Figure 9, are produced by adjusting the values of k_o , k_i , and k_e to reflect each habitat's exclusive availability. We begin with the all-

outdoor balance, where $k_o = 1 \text{ m}^2$ and $k_i = k_e = 0$, then consider the all-indoor case, where $k_i = 1 \text{ m}^2$, $k_o = k_e = 0$, and the all-enclosed case, where $k_e = 1 \text{ m}^2$, $k_o = k_i = 0$. While all constant and temperature-dependent parameters in the model take on the values previously established, adjusting the levels of available aquatic habitat changes the migration rates and wet egg laying proportions as specified in Table 1. In Table 2, we list the resulting values for each of these parameters. We use these conditions to plot the outdoor, indoor, and enclosed adult populations over five years in each scenario.

Table 2. Migration and wet laying rates by exclusively available habitat type

Habitat	m_{2io}	m_{2oi}	m_{2oe}	p_{wo}	p_{wi}	p_{we}
All outdoor	$\frac{\alpha}{l_v}$	0	0	.91	0	1
All indoor	0	$\frac{\alpha}{l_v}$	0	0	.91	1
All enclosed	0	0	$\frac{\alpha}{l_v}$	0	0	1

After producing population graphs for the three most extreme habitat cases, we examine the more realistic situation in which portions of outdoor, indoor, and enclosed habitat appear simultaneously. We vary the outdoor and indoor aquatic habitats from 0 to 1 m^2 by increments of $.2 \text{ m}^2$, such that their sum never exceeds a constant total area of 1 m^2 , and set the enclosed habitat equal to 1 m^2 less the sum of the other two habitat areas. For each of the 21 resulting habitat combinations, we again plot the total adult population over the course of five years, allowing enough time for the system of equations to reach a periodic solution. We visualize the results of these simulations in three heat maps, where the first shows the annual peak adult population given each habitat balance and the second shows the annual minimum adult population. These values are computed by using the plotting tool in MatLab to find the highest and lowest values reached annually along the periodic portion of each solution curve. For the third heat map, we use the trapezoidal numerical integration feature in MatLab to calculate the area under each solution curve over one year once periodicity is reached, describing the total annual adult population. Doing so allows us to determine the optimal distribution of habitats within a fixed aquatic area: the balance that leads to the highest total count of annually emerging adults.

Having determined the optimal balance of outdoor, indoor, and enclosed habitats to maximize the annual adult population in El Paso, we conclude the first set of simulations by plotting the outdoor, indoor, and enclosed populations under the ideal conditions for population maximization. We compare the proportions of adults appearing in each habitat and present our conclusions regarding optimal habitat distribution.

4.2 Comparing Outdoor Survival Among Regions

Although the first set of simulations demonstrates the optimal habitat balance given El Paso’s weather conditions, these results stand to vary in regions with differing temperature patterns. Our second simulation explores the effects of climate variation on vector viability. Monaghan et al. produce maps of the range of *Aedes aegypti* in the United States based on the Skeeter Buster model and report the vector’s prevalence in fifty major cities within this area (Monaghan et al. 2016). To quantify the results of this study using our own modeling methods, we select a city from each reported level of vector prevalence risk and evaluate the range of *Aedes aegypti* adult population levels over several years in each environment. In addition to El Paso, which falls at the lower end of the scale of reported risk, we investigate Minneapolis, New York, New Orleans, Orlando, and Miami, which ascend in peak vector risk from non-existent to moderate to high. Table 3 lists the study’s qualitative reports of the vector prevalence risk in each city, as well as the average maximum and minimum temperatures in each region.

Table 3. Average temperatures and reported vector prevalence in six U.S. cities (from Monaghan et al. 2016)

City	Jan. Vector Risk	July Vector Risk	Jan. Avg. Temp. (°C)	July Avg. Temp. (°C)
Minneapolis, MN	None	None	-9.1	23.2
El Paso, TX	None	Low	7.3	28.2
New York, NY	None	Moderate	0.4	25.2
New Orleans, LA	None	High	11.9	28.5
Orlando, FL	Low	High	15.7	28.7
Miami, FL	Moderate	High	20.1	29.0

In order to assess vector risk levels in the six regions, we first fit a temperature model for each city using the same Fourier function that we initially fit to El Paso’s climate. In Figure 8, we plot average temperatures over two years in each of the six cities along with the equilibrium

viability range, which is overlaid in white along the middle of the temperature spectrum. The range of equilibrium viability aligns closely with the risk levels reported by Monaghan et al. In Minneapolis, New York, El Paso, and New Orleans, where winter temperatures fall below the lower viable bound for several months of the year, Monaghan et al. report no risk of vector prevalence in January. In Orlando, where the lowest temperature falls on the border of the viable range, winter vector prevalence is low. In Miami, temperatures remain within the optimal range for vector survival at all times, and a moderate to high year-round population is anticipated. For July, when vector risk levels peak, all cities except New York and Minneapolis reach temperatures between 28°C and 29°C. Monaghan et al. report that Minneapolis, which reaches the lowest peak temperature and remains below the viable range for the largest portion of the year, is never at risk for *Aedes aegypti*. We draw on the finding that Minneapolis is not expected to have adults present at any time to treat the region as a control in our simulations.

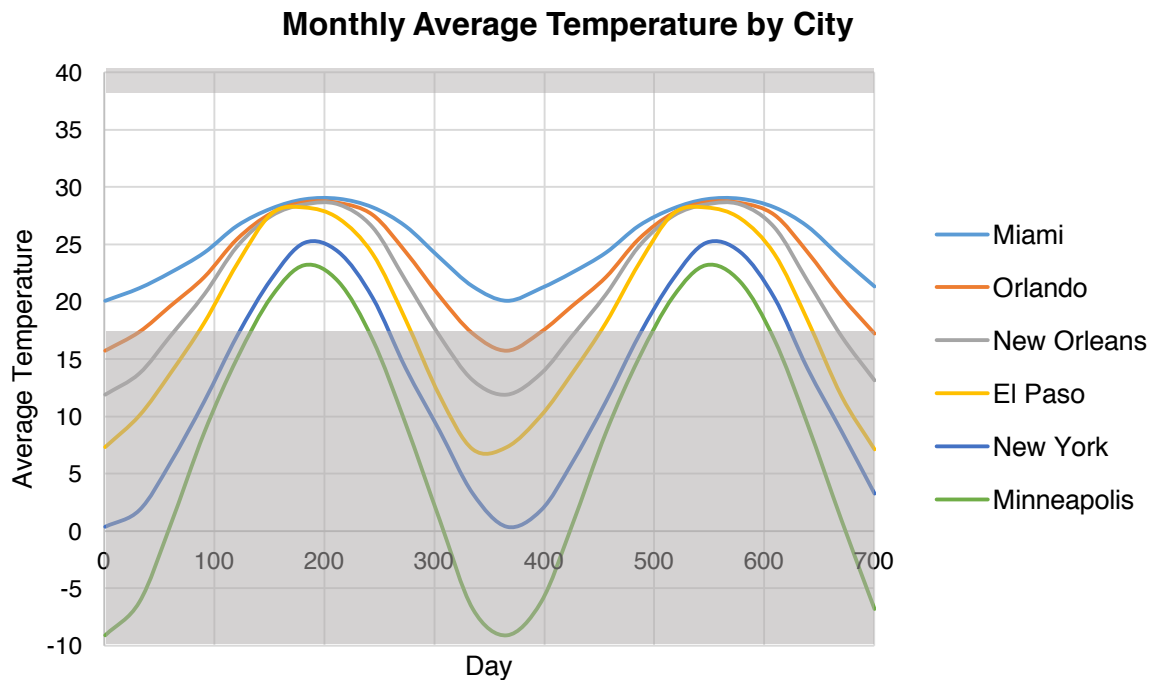


Figure 8. Average monthly temperatures over two years for six U.S. cities. Each line represents two iterations of one year of monthly average temperatures for the specified region. The overlaid gray area represents temperatures falling outside of the range of equilibrium viability, which spans from 16.16°C and 38.33°C.

After assigning temperature models to all six regions, we investigate the five cities that are reported to have some level of persistent vector risk—El Paso, New York, New Orleans, Orlando, and Miami—anticipating that these regions will foster consistent survival rates and high summer population levels. We simulate five years of population fluctuations in each region given a constant outdoor wet habitat area of 1 m² and no indoor or enclosed habitat. In addition to setting the indoor and enclosed habitat areas equal to zero as in the initial exclusively outdoor simulation in Section 4.1, we assign 0% migration rates during both feeding and laying among all habitats. Doing so prevents feeding adults from migrating into the indoor habitat in search of human subjects and ensures that the population exists entirely outdoors. Figure 13 shows the resulting population levels for these five initial simulations. The plot for each city shows fluctuations in its outdoor adult population over five years, during which period all five climates lead to periodic solutions.

Next, we investigate Minneapolis to determine whether our model’s predictions match the expectation that the vector population will not survive there over the course of the five-year period. We run an initial simulation of population levels in this climate following the same procedure as in the other five cities. We additionally recall that dry egg flooding rates are a driving factor for adult survival, as a large dry egg population is a means of improving population viability during the winter (Sota and Mogi 1992). To evaluate the effects of this parameter, we vary the flooding rate by increments of .01 between 0 and .14, and then by increments of .1 up to 1, and calculate the total annual adult population under each flooding condition. As in the third heat map, we take the annual adult population as the sum of the area under the solution curve over 365 days once the population level has reached periodicity. This simulation allows us to determine three brackets of flooding rates, which we describe as under-flooding, viable flooding, and over-flooding, for Minneapolis. We select a rate within each category and model population levels in all eight life stages over the course of five years for each rate, allowing us to more closely investigate the influence of flooding rates on population dynamics.

4.3 Evaluating the Impact of Indoor Habitat

Simulating adult population levels under varying U.S. climate conditions indicates contrasts among regions in which the vector can reliably survive year-round and those in which

its re-emergence occurs only in the summer months or in the presence of optimal dry egg flooding conditions. Given the level of variation among cities in each of these categories, the re-introduction of the possibility of migration into climate-controlled indoor habitats has a distinct effect on the vector population in each case. In the third set of simulations, we analyze the impact of indoor habitat availability in three regions to understand to what extent the redistribution of habitat into climate-controlled spaces changes the size of the adult population in each type of climate.

We select Minneapolis, New Orleans, and Miami as three sample cities for this simulation. In Minneapolis, the coldest of the three regions, temperatures fall below the indoor level of 21°C for most of the year, and indoor environments are expected to present more optimal temperature conditions than the outdoor habitat in the winter. New Orleans offers warmer outdoor conditions than Minneapolis, with temperatures falling above and below 21°C for roughly equivalent portions of the year. There, migrating indoors remains a more optimal possibility than remaining outdoors in the winter, but summer temperature conditions are generally more favorable outdoors than inside buildings. Finally, in Miami, where outdoor temperatures are almost always greater than the designated indoor level, we anticipate that migrating indoors to feed or lay will not have a positive effect on the vector population.

Having selected three cities in which we believe that the presence of indoor spaces presents varying opportunities for the augmentation of survival viability, we run five-year simulations of the outdoor, indoor, and enclosed adult populations in each area. We maintain a total habitat area of 1 m² and a balance of .8 m² outdoor, .2 m² indoor, and no enclosed habitat to follow the ideal conditions derived for El Paso in the first simulation. However, we recognize that this habitat balance does not necessarily maximize the adult population in every climate. We evaluate outcomes in each city by comparing the total annual outdoor population without migration to the total annual outdoor population in the case with 20% indoor habitat. Finally, we present our conclusions regarding the difference in impact of indoor habitat among climates.

5. Results

The numerical experiments specified in Section 4 allow us to determine optimal habitat distribution and compare the effects of habitat variation among U.S. cities with distinct temperature patterns. In this section, we use model simulation results to report the adult *Aedes aegypti* population's response to shifting climate and habitat conditions. In Section 5.1, we evaluate the changes in population levels that result from varying the available proportions of outdoor, indoor, and enclosed habitat. In Section 5.2, we analyze annual vector prevalence in outdoor habitats in six U.S. cities and compare predicted population levels with the Skeeter Buster model's findings regarding vector survival in each region (Monaghan et al. 2016). Finally, in Section 5.3, we re-introduce the possibility of migration to indoor environments to show how the presence of climate-controlled habitat leads to new potential for vector survival.

5.1 Habitat Balance

As a first simulation, we maintain a constant total habitat area with El Paso's temperature conditions and adjust the proportion of this area that each type of habitat comprises. The three initial outcomes in Figure 9 show the daily adult population over the course of five years when this habitat is entirely outdoors, entirely indoors, and entirely enclosed.

When the available wet habitat is exclusively outdoors, the population peaks each summer and more adults inhabit the outdoor habitat than any other environment. The vector does not migrate into enclosed spaces in the absence of wet enclosed habitat for laying, but migration into the indoor habitat does occur, as feeding on humans in indoor spaces remains a possibility. The total annual adult population among all three habitats, measured as the area under all three solution curves summed over 365 days, is 2600 mosquitos, reflecting the vector's ability to survive well under warmer conditions despite dying out in the winter of each year. Conversely, when the available habitat is entirely indoors, the vector survives year-round at a lower total population. In line with the equilibrium population level for 21°C shown in Figure 7, there remains a constant daily population of about 5 adults, and the total annual population is around 2000. These initial outcomes suggest that a higher proportion of outdoor habitat maximizes the vector population, while a higher proportion of indoor habitat is optimal for year-round survival.

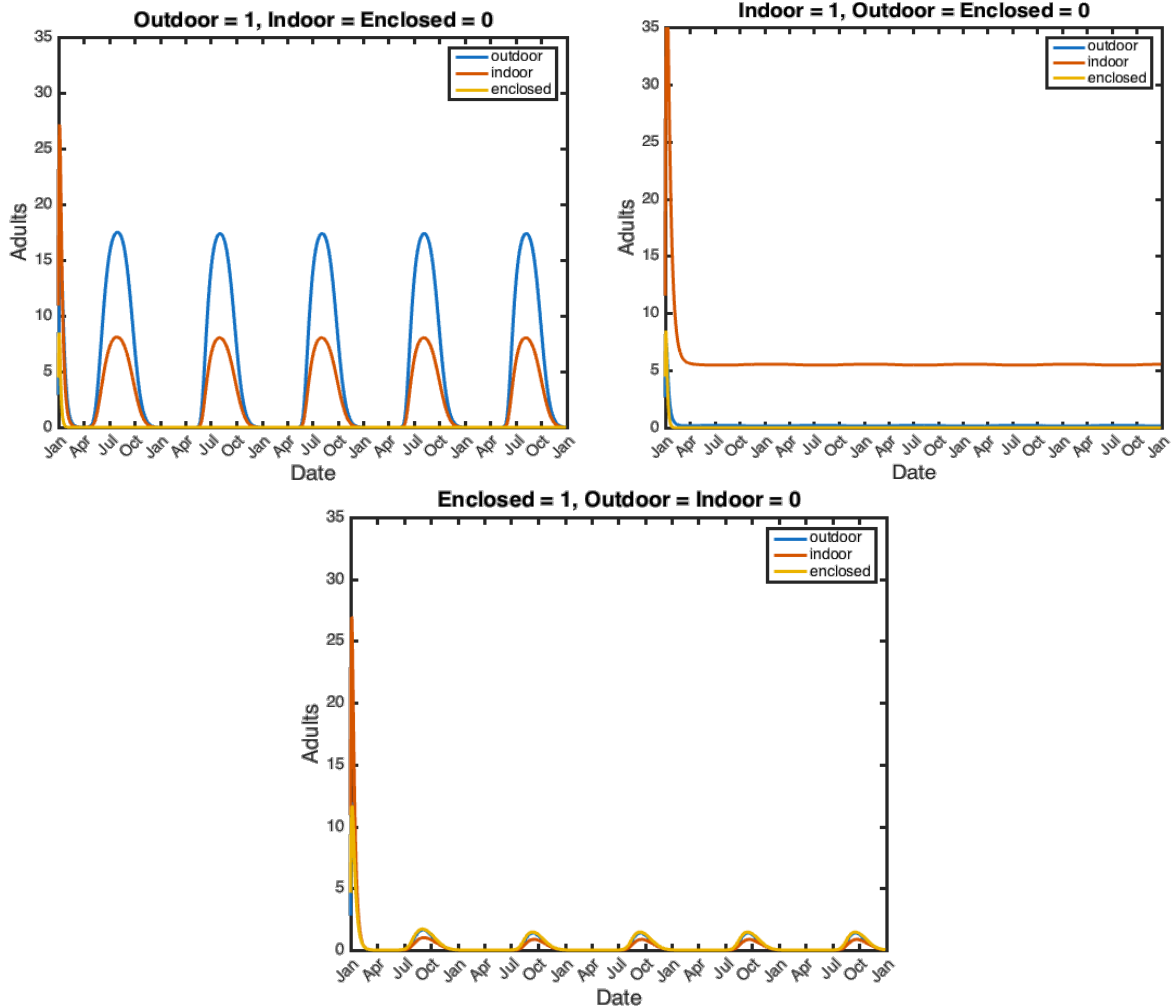


Figure 9. Daily adult population by predominant habitat type in El Paso, TX. In each simulation, the blue curve represents the daily adult population in the outdoor habitat, the orange represents the indoor habitat, and the yellow represents the enclosed habitat. Aquatic area is restricted to 1 m² and appears entirely in one habitat in each case.

The case in which wet habitat is only available in enclosed spaces is least optimal for vector survival. With only enclosed habitat available for laying, adults must migrate outdoors, and potentially subsequently enter indoor spaces, in order to find human subjects for feeding. This pattern reduces the efficiency of the gonotrophic cycle, and the total population consequently remains low. Because enclosed spaces are also insulated, and therefore delayed in reaching peak temperatures, the total population peaks later in the year in this scenario. Given the suboptimal conditions for survival in enclosed habitats, the total annual population in this case is much smaller than the populations appearing in exclusively indoor or outdoor environments, only reaching about 300 adults.

While the three aforementioned situations represent extreme examples of habitat balance, it is unlikely for only one type of habitat to be available at any given time. The following heat maps show the population levels that result when the proportions of the three habitat types are varied given constant total habitat area. The horizontal axis represents the proportion of habitat that appears outdoors, the vertical represents the indoor proportion, and the enclosed proportion is set at 1 m^2 less the sum of these areas. The maximum population map reports the sum of the outdoor, indoor, and enclosed adult populations at their peak levels, which typically occur in July, given each habitat ratio. The minimum map shows the lowest annual population level for each scenario.

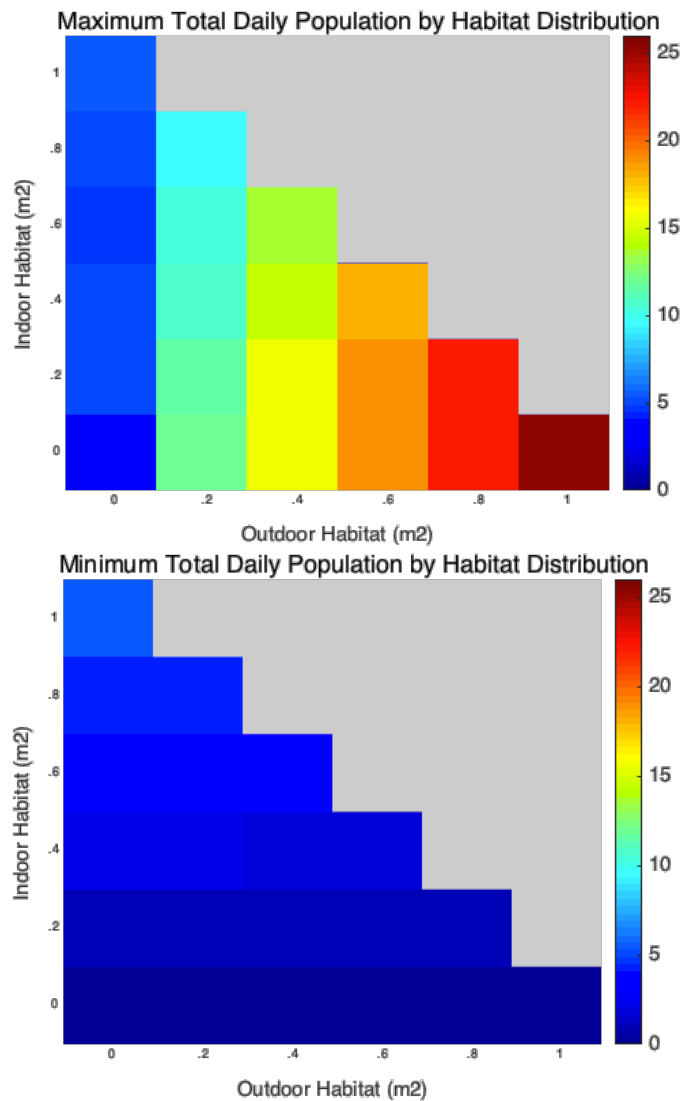


Figure 10. Annual maximum and minimum total adult populations by habitat balance in El Paso, TX. In each heat map, outdoor, indoor, and enclosed areas are varied by increments of $.2 \text{ m}^2$ to maintain a constant total area of 1 m^2 . The first map shows the highest population level and the second shows the lowest, calculated as the maximum and minimum values of the solution curve, respectively, once periodicity is reached.

The trends in these heat maps match the simulation results in Figure 9. While the maximum annual population is highest when the available habitat is entirely outdoors, the vector cannot survive year-round in the absence of indoor habitat. Consequently, the highest maximum populations correspond to the lowest annual minimum populations. In order to understand which habitat ratio maximizes the total vector population appearing annually, we integrate the outcomes corresponding to each habitat ratio over the course of one year. Figure 11 shows the resulting population levels.

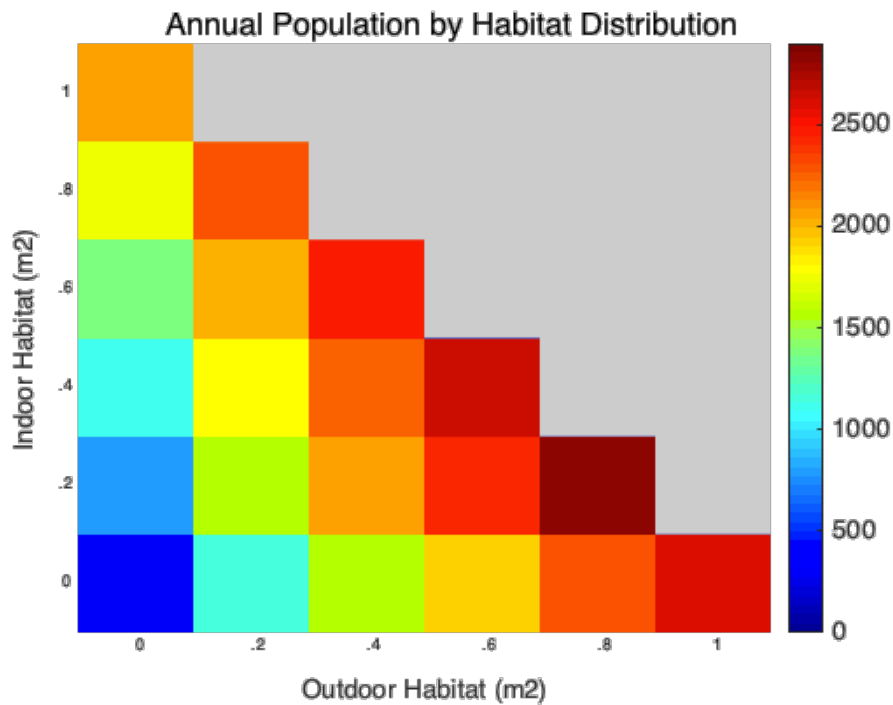


Figure 11. Total annual adult population by habitat balance in El Paso, TX. Population levels are determined given the same habitat distribution patterns as in Figure 10. In each case, the total annual adult population is calculated as the sum of the area under the solution curve over 365 days once periodicity is reached.

The annual population totals affirm the trade-offs between habitat ratios that maximize population levels and those that optimize year-round survival potential. The maximum total population appears when the square meter of available habitat includes 80% outdoor area, 20% indoor area, and no enclosed area. Population levels decrease along each subsequent diagonal, indicating that emergence rates become lower with increasing levels of enclosed habitat. The negative effect of additional enclosed habitat on population totals reflects the inefficiency of breeding in an environment in which there are no human subjects for feeding. Regardless of the level of enclosed habitat, however, peak total populations tend to appear along the 20% indoor

habitat level. As Figure 12 shows, re-introducing 20% indoor habitat to the entirely outdoor model for El Paso allows the vector to survive indoors at a low level year-round without drastically reducing the annual peak populations. This adjustment produces the optimal balance among those explored for maximizing both population levels and survival potential.

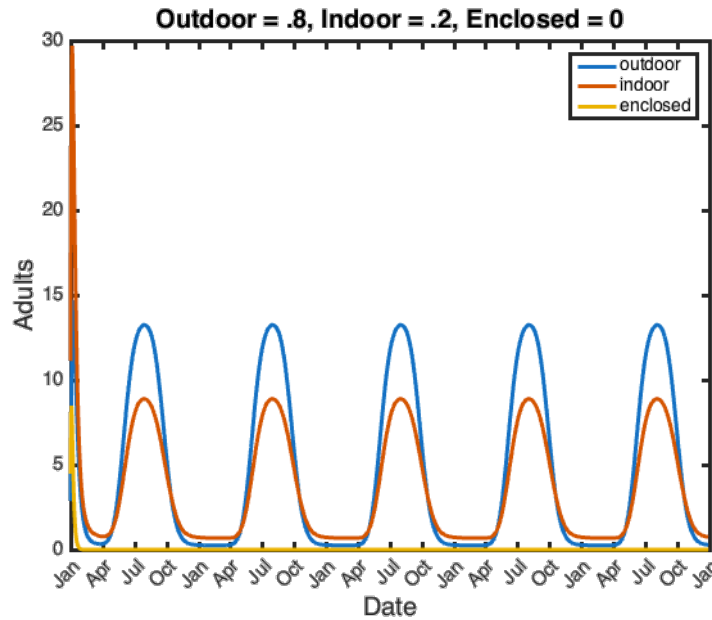


Figure 12. Daily adult population in El Paso, TX with habitat types balanced to maximize annual population totals. Habitat distribution is set to 1 m² appearing 80% outdoors and 20% indoors. Outdoor, indoor, and enclosed solution curves appear in the same colors as in previous simulations.

Several conclusions on habitat balance arise from our exploration of the proportions of available outdoor, indoor, and enclosed habitat in El Paso. First, when the total available habitat appears exclusively in one type of environment, an all-outdoor habitat is conducive to maximum peak population levels, while an all-indoor habitat ensures year-round survival. An exclusively enclosed habitat supports the lowest number of total adults and creates low peaks that last for only a small portion of each year. When mixed habitat types are introduced, models in which 20% of the habitat appears indoors both ensure year-round survival and maximize annual population totals in El Paso. These habitat balance findings reflect the optimality of being exposed to high outdoor summer temperatures and being able to seek shelter in climate-controlled indoor habitats in the winter, as well as the inefficiency of breeding in enclosed spaces with no human inhabitants. Nevertheless, emergence and habitat patterns stand to vary in climates that differ from El Paso’s, which the following simulations investigate.

5.2 Outdoor Viability by Region

The initial simulation results affirm that *Aedes aegypti* adults cannot survive year-round outdoors in El Paso, where temperatures fall below the optimal range for much of the year. To explore how this outcome changes among climate types, we compare El Paso with five other U.S. cities with varying weather conditions and levels of vector viability. Figure 13 shows the periodic solutions that result over five years when the system of equations is evaluated under the climate conditions of New York, El Paso, New Orleans, Orlando, and Miami.

The outdoor habitat outcomes in the first five cities generally match expectations drawn from both the equilibrium viability range and the values reported in Monaghan's study. During peak vector season, we witness minimal distinctions between New Orleans, Orlando, and Miami, which are designated as high-risk; all three cities support peak daily populations of just under 30 adults per square meter of aquatic habitat. These three regions also have similar peak summer temperatures of 28.5°C to 29°C, affirming that the maximum vector population reached in each region is closely related to its maximum annual temperature. Peak population levels for New York and El Paso coincide to a lesser degree with Monaghan's study, which indicates a larger presence of *Aedes aegypti* adults in New York than in El Paso. However, the relative maximum population levels of the two cities are logical given that both summer and winter temperatures are warmer in El Paso than in New York. El Paso's maximum temperature and vector population are both close in value to those of the warmest three cities, whereas New York's lower population peaks reflect more temperate summer weather and the difficulty of full recovery from cold winter conditions.

At colder temperatures, differences in risk levels among geographical locations are also clear. El Paso, New York, and New Orleans have no adults present between January and April, true to the reported non-existent risk level and the relatively long periods during which the temperatures of all three regions fall below the lower bound of equilibrium viability. In Orlando, the population falls just above the threshold for being present year-round, corresponding to a reportedly low winter risk and a minimum temperature that lies on the lower equilibrium limit. Finally, as predicted, *Aedes aegypti* adults are present in Miami during even the coldest months of the year, though the population still fluctuates annually in response to changes in temperature.

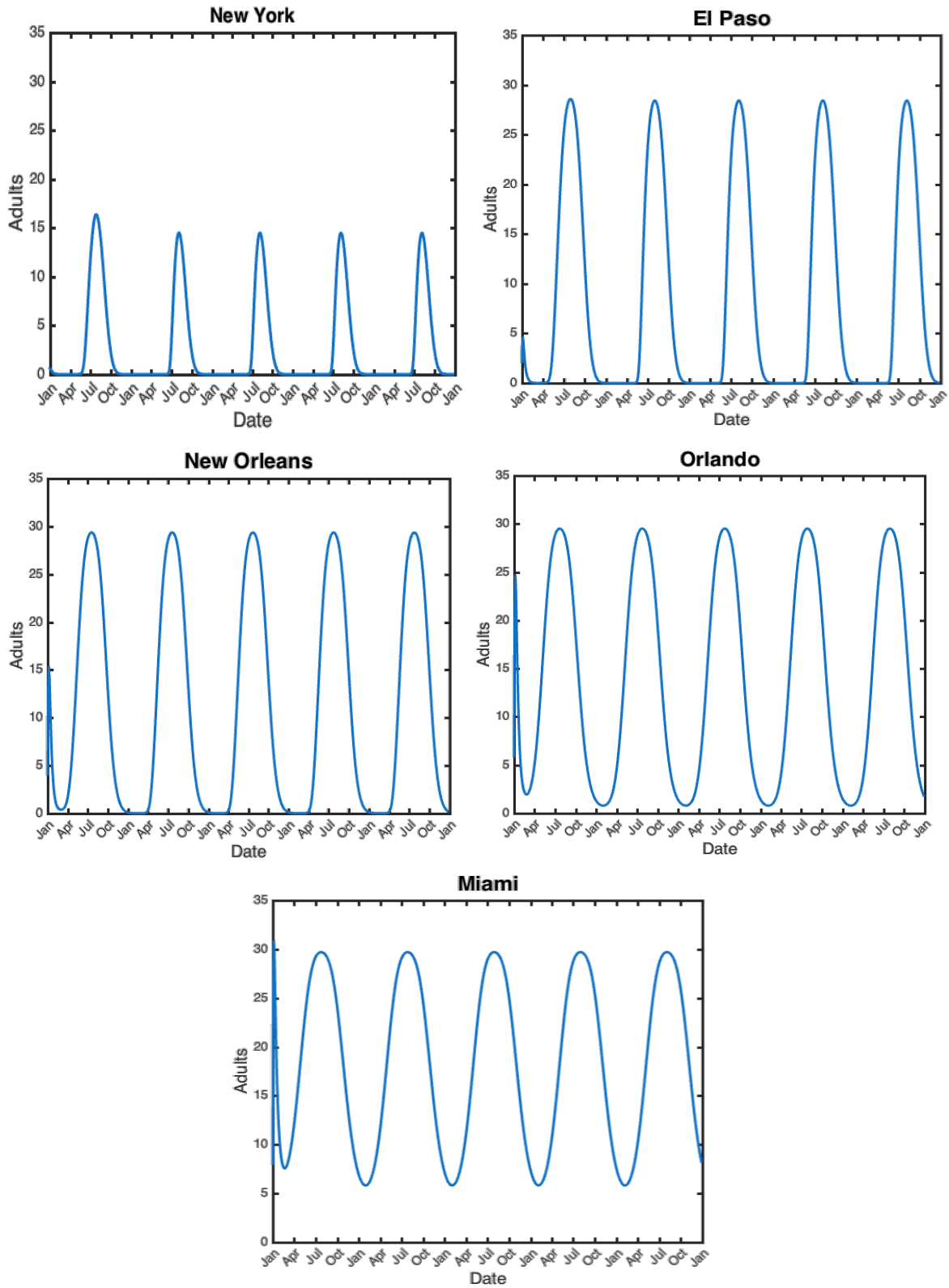


Figure 13. Outdoor population levels by U.S. city in the absence of migration. Each simulation shows population dynamics over five years for 1 m² of exclusively outdoor aquatic habitat governed by the climate model corresponding to the designated city. All migration rates during feeding and laying are set to zero to remove the possibility of departure to other habitats.

In Minneapolis, survival of *Aedes aegypti* adults is highly unlikely due to winter temperatures that fall far below the vector's optimal climate range. Because *Aedes aegypti* has never been reported to live in the region, we anticipate that the population will die out rather than reappearing annually. However, as Figure 14 shows, a five-year simulation for Minneapolis with the initially established model parameters reaches a periodic solution at which the vector is present for about a quarter of each year.

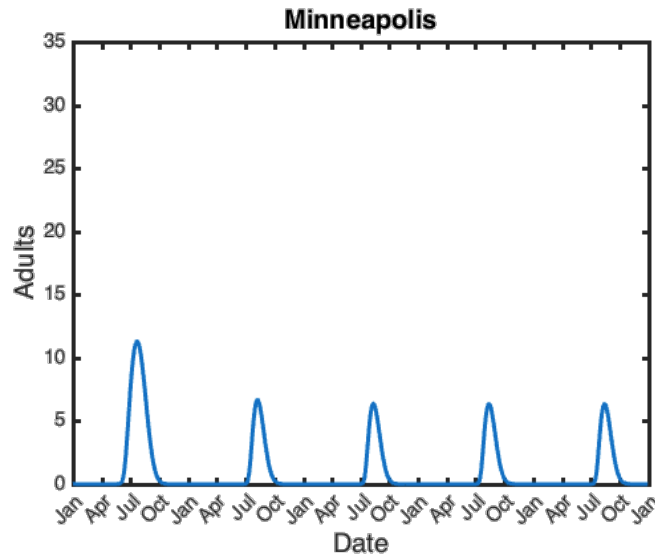


Figure 14. Outdoor population dynamics over five years in Minneapolis, MN with persistent survival. Given the initial dry egg flooding rate, the vector re-emerges each year between July and October rather than dying out as anticipated by previous modeling and observations.

This simulation result suggests that the conditions present in the model are more conducive to cold season survival than the preexisting literature anticipates. Given that eggs are the primary subpopulation remaining viable in the winter months, we investigate the balance of eggs laid in wet and dry areas as a potential factor explaining the unprecedented survival of adults (Sota and Mogi 1992). We first investigate the flooding rate, which determines the transition of eggs from the dry to the wet stage and consequently influences the number of eggs appearing in each cohort at a given time. While the initially assumed human-driven flooding rate of .071 produces the above periodic solution, as we vary this rate between zero and one, the adult population does not consistently reemerge annually. Figure 15 shows the total annual adult population in an exclusively outdoor habitat of 1 m² in Minneapolis, with no possibility of migration, by egg flooding rate.

Annual Adult Population by Flooding Rate, Minneapolis

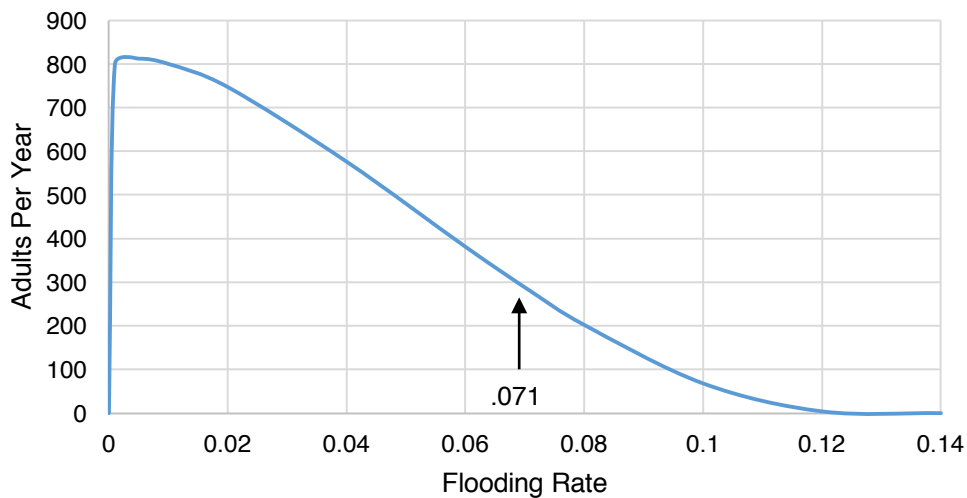


Figure 15. Total annual adult population in Minneapolis, MN by dry egg flooding rate. When the flooding rate is zero or above .12, the population dies out after one year and the sum of the area under each subsequent year’s solution curve is zero. Between these rates, the population is able to re-emerge annually at the total levels displayed.

An analysis of the adult population by flooding rate affirms that the initial value of .071 falls within a small range of flooding rates in which the adult population is able to reappear annually. When no flooding takes place, the adult population remains at zero, reflecting the vector’s inability to survive persistently when dry eggs lose viability without ever entering a wet state. However, the introduction of even a very small flooding rate of .001 supports an annual population of over 800 adults per square meter of aquatic habitat. The population level subsequently declines as flooding rates increase, before again reaching zero by the maximum displayed flooding rate of .14. That is, the daily flooding of 1/7 or more of the dry egg population precludes the ongoing survival of *Aedes aegypti* adults in the Minneapolis climate.

Although it initially seems that adult survival should become more viable, rather than less likely, as flooding rates increase, the disappearance of the adult population beyond a flooding rate of about .12 is not unjustifiable. Dry eggs serve as a valuable subpopulation for the insurance of long-term survival in cold climates, as the eggs can remain viable without freezing or hatching into larvae as wet eggs do (Eisen et al. 2014). Once wet eggs enter the small larva stage, they become subjected to temperature-dependent mortality rates, which lead to a depletion of the population in conditions as unfavorable as Minneapolis’ winter climate. However, if eggs remain dry for longer periods, only being flooded into the wet cohort in small groups, it is more

possible for a subgroup of the population to survive through the coldest months. Our findings on the effects of flooding rates reflect the importance of oviposition in dry environments as a means of breeding sustainably under suboptimal climate conditions.

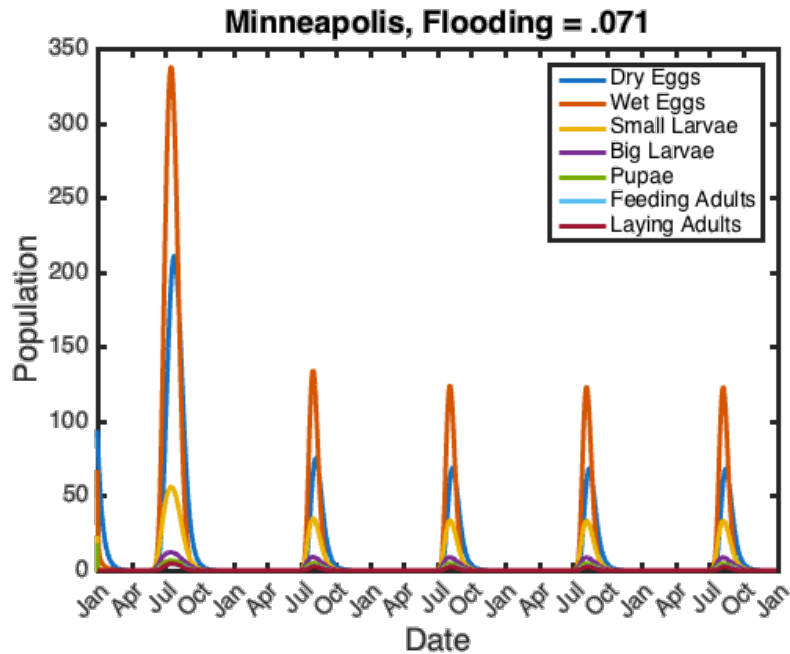


Figure 16. Population by life stage in Minneapolis, MN with the initial flooding rate of .071, at which annual re-emergence is viable. Wet eggs are the maximum subpopulation each year, followed by dry eggs, small larvae, big larvae, pupae, and feeding and laying adults. The third adult stage is not shown because of its irrelevance to the gonotrophic cycle.

In Figures 16 and 17, we simulate fluctuations in all life stages over the course of five years with a flooding rate that is conducive to ongoing survival, .071, and then with under- and over-flooding at rates of 0 and .14. In the sustainable flooding case, wet eggs remain the highest subpopulation at all times, followed by dry eggs and the subsequent life stages. This ratio of subgroups matches the over-flooding case, in which wet eggs remain most prominent until the entire population dies out at the end of the first year. In the under-flooding scenario, however, when there is no means of transition from the dry to the wet state, the dry egg population survives at the highest rate of the eight life stages until all dry eggs lose viability after about two years. The ratios of dry to wet eggs at each flooding rate provide additional affirmation of the importance of a rate that does not lead to overpopulation of either group.

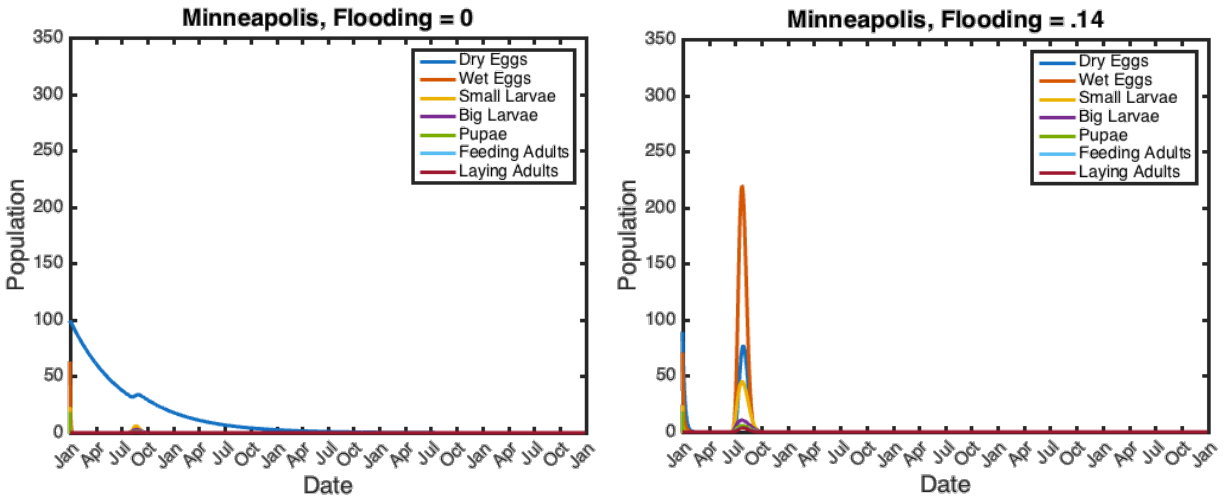


Figure 17. Population by life stage in Minneapolis, MN with flooding rates of 0, representing under-flooding (left) and .14, representing over-flooding (right). No subpopulation re-emerges after the first year in either case. Wet eggs remain the largest subgroup with over-flooding, while dry eggs have the largest population with under-flooding.

In this series of simulations by geographical region in the absence of indoor and enclosed habitats, Monaghan’s study of seasonal risk guides our selection of six U.S. cities with varying vector population levels. Across most cities, reported qualitative risk aligns with temperature patterns and simulation outcomes; regions with reportedly non-existent January risk and low winter temperatures are not shown to sustain an adult *Aedes aegypti* population for the entirety of the year, while those with tropical climates and moderate to high risk support the ongoing survival of the vector population. Our analyses of El Paso, New York, New Orleans, Orlando, and Miami affirm these trends. Minneapolis is anomalous in that it has never been observed or reported to be at risk for *Aedes aegypti*, yet the model’s initial parameters lead to annual reemergence of the population. We find that this trend is contingent on the flooding rate of dry eggs falling within a small range, suggesting that oviposition in dry habitats may be a viable outdoor survival tactic in a wider geographical range than previously anticipated.

5.3 Effects of Indoor Habitat Re-Introduction

Simulating population levels in exclusively outdoor habitats reveals that of the U.S. regions considered, only southern Florida supports the year-round survival of *Aedes aegypti* adults. However, the habitat ratio analysis in Section 5.1 affirms that an entirely outdoor habitat structure neither fosters year-round survival nor maximizes the emerging adult population; both

results are most reliably achieved through the introduction of indoor habitat. Accordingly, we simulate the re-introduction of indoor habitat to three regions with varying outdoor survival viability: Minneapolis, where *Aedes aegypti* cannot reliably survive, New Orleans, where the vector consistently reemerges but adults are not present year-round, and Miami, where tropical temperatures facilitate year-round outdoor survival. We establish a balance of 20% indoor and 80% outdoor habitat in each region, again with a fixed total area of 1 m^2 , based on the optimal outcome observed for El Paso in Section 5.1. Model parameters otherwise remain as specified in Section 2.

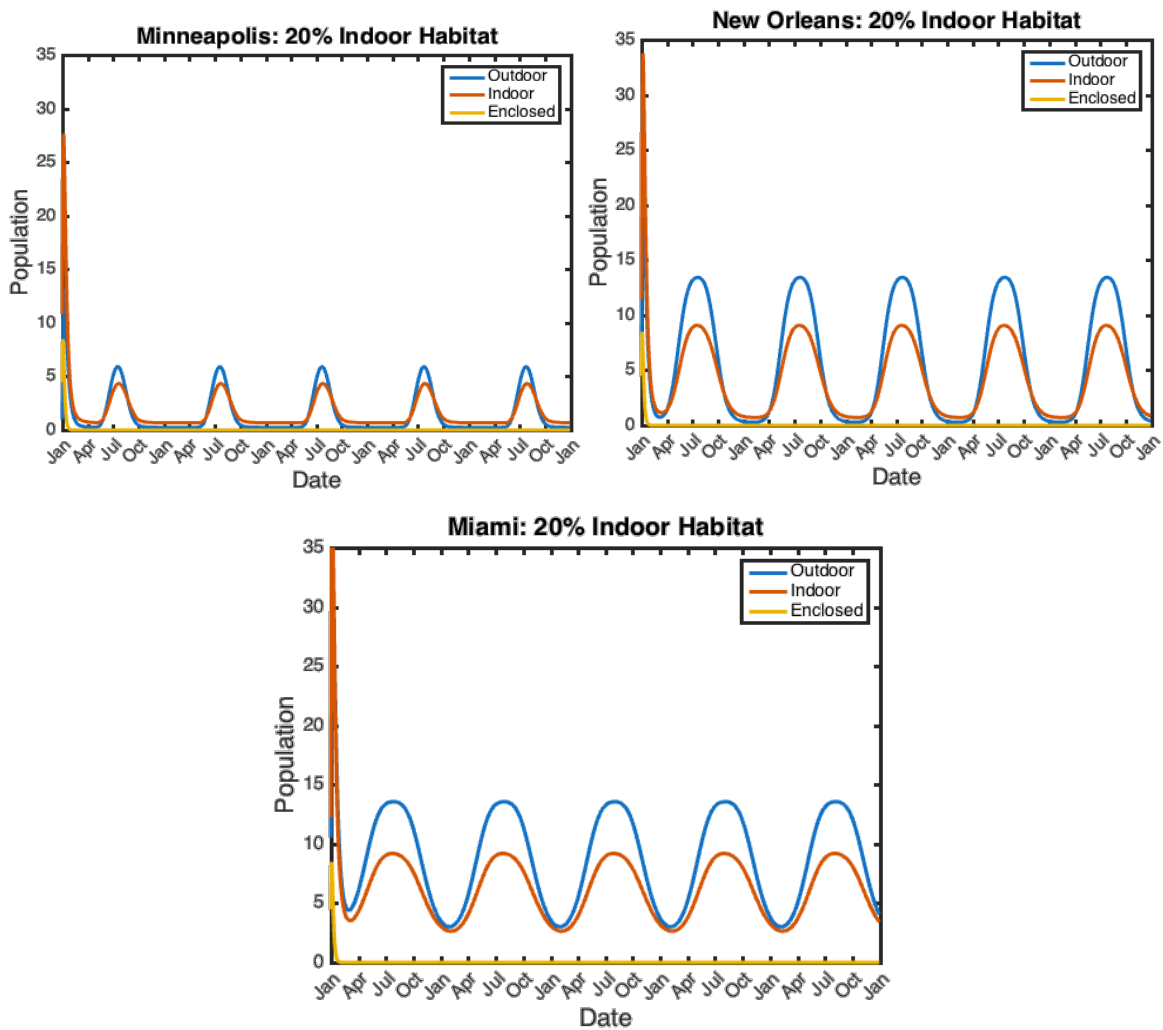


Figure 18. Impact of indoor habitat re-introduction in Minneapolis, MN, New Orleans, LA, and Miami, FL, three cities with varying levels of annual vector viability. Outdoor, indoor, and enclosed populations are plotted over five years with the optimal El Paso habitat balance of $.8 \text{ m}^2$ outdoor habitat and $.2 \text{ m}^2$ indoor habitat.

The redistribution of outdoor habitat to indoor spaces produces varying effects across regions and climates. In Minneapolis, the outdoor population in Figure 18 peaks at the same level each summer as in the exclusively outdoor case, and an indoor cohort of nearly that size also emerges annually. The total annual population increases to over a thousand adults with the re-introduction of indoor habitat, nearly quadrupling the value it reaches in the entirely outdoor case. Although the population still effectively disappears each winter, with less than one mosquito predicted to occupy each habitat, the presence of indoor breeding area generally improves conditions in Minneapolis in terms of both the length of time that the vector is present and the total number of adults that the habitat can support.

Table 3. Total annual adult population in all habitats in three cities by habitat balance

City	Population, 100% Outdoor	Population, 20% Indoor 80% Outdoor
Minneapolis, MN	279	1010
New Orleans, LA	3998	3420
Miami, FL	6064	5292

In New Orleans, incorporating indoor aquatic habitat slightly increases the total annual adult population and ensures non-zero winter survival. While the overall yearly population increases by about 500 adults, summer peaks are reduced when a portion of the available habitat appears indoors and migration becomes a possibility. Rather than the maximum population of 30 adults per square meter that emerges in the entirely outdoor case, the New Orleans climate supports a peak of about 10 adults indoors and 13 outdoors per square meter of total aquatic habitat. The longer period of survival and larger winter population in both habitats compensate for these lower peaks in the total population counts.

Unlike in New Orleans and Minneapolis, however, moving a portion of the available habitat indoors in the model for Miami does not improve conditions for the vector population. *Aedes aegypti* adults can still definitively survive year-round in Miami in the 20% indoor habitat case, but both the summer peak levels and the total annual population are reduced. This outcome aligns with our findings on equilibrium population levels by temperature. In Miami, where outdoor temperatures remain above the indoor level of 21°C for all months except January, outdoor climate conditions are more favorable to the vector population than indoor spaces for nearly all of the year. We conclude from this simulation that, given a fixed total aquatic area,

migration to indoor habitats is most helpful for vector survival in cold climates, while it lowers population levels in environments that already support year-round survival of *Aedes aegypti* adults. However, these results stand to differ when total habitat area is not fixed: Population outcomes would be more favorable for *Aedes aegypti* adults across regions if the indoor habitat were to appear in addition to, rather than instead of, the existing outdoor area.

6. Discussion

In this study, we develop a model describing temperature-dependent fluctuations in the population of *Aedes aegypti* and evaluate the vector's growth and survival under varying climate and habitat conditions. Given the severity of symptoms and lack of vaccines for the four primary diseases that *Aedes aegypti* transmits, analyzing mosquito population dynamics is now a particularly important means of guiding disease prevention through vector control. While previous studies have proposed models reflecting the vector's temperature-dependent lifecycle, this project uniquely incorporates egg desiccation, migration among three distinctly defined habitats, and a new geographical area of focus to consider the effect of manmade habitats on vector viability in the United States. The application of our system of differential equations to outdoor, indoor, and enclosed habitats in six cities allows us to determine the regions and habitat distributions that are most conducive to vector survival.

After establishing our system of 23 ordinary differential equations, which account for eight life stages in the outdoor and indoor habitats and seven life stages in enclosed areas, we analyze temperature-dependent population dynamics by evaluating the range of constant temperatures at which the population can viably reach equilibrium. Our finding that equilibrium is viable between approximately 16°C and 38°C, which we calculate according to Descartes' Rule of Signs, informs our subsequent evaluations of the survival potential of *Aedes aegypti* adults in the U.S. cities of interest. We begin by examining habitat balance in El Paso, TX. We simulate population levels in the three possible cases of habitat homogeneity and then compare the total yearly populations across a range of habitat distributions to conclude that the number of annually emerging adults is maximized when the square meter of total habitat appears 80% outdoors and 20% indoors. Beyond demonstrating the optimal habitat balance for *Aedes aegypti* adult survival, this simulation reaffirms that vector control is best achieved by minimizing the available outdoor aquatic habitat in the summer and emptying indoor water receptacles at colder temperatures.

Given the variation in climate among regions of the United States, we move beyond El Paso to explore the effects of temperature and habitat on population dynamics in five other U.S. cities. We draw upon Monaghan's 2016 study and the equilibrium viability range to select regions whose climates represent distinct levels of suitability for vector survival, which range

from Minneapolis, MN to Miami, FL. In line with both temperature patterns and Monaghan's risk level predictions, we witness low survival rates in Minneapolis that are contingent on optimal flooding, year-round survival in Miami, and a combination of summer peaks and winter disappearance in the remaining cities. Recognizing that these results stand to change in the presence of indoor and enclosed habitats, we redistribute a small portion of the total aquatic area to indoor spaces in Minneapolis, New Orleans, and Miami. We find that moving a portion of the total habitat to climate-controlled indoor spaces increases the adult population's total size and chance of survival in cold climates. However, when total habitat area is fixed, redistributing a portion to indoor spaces reduces the number of emerging adults in a region such as Miami with a highly favorable outdoor climate.

While we are able to validate many of our findings on the vector's range and population levels against preexisting reports, our results diverge from the literature in a few areas. The Skeeter Buster model cited in Monaghan et al. predicts higher vector risk in New York than in El Paso and shows no survival viability beyond a narrow swath of the southern and eastern United States (Monaghan et al. 2016). In our simulations, we find that the climate of southern Texas supports both a longer annual period of *Aedes aegypti* survival and higher population peaks than that of New York City. Furthermore, while we initially select Minneapolis as a region that cannot support a nonzero vector population based on Monaghan's findings, our model shows a small annually re-emerging *Aedes aegypti* adult population given an optimal balance of wet and dry eggs. Particularly with the incorporation of indoor and enclosed habitats, our model tends to show a broader range of viability than has previously been modeled or observed in the United States.

Various sources of error influence these results. The temperature-dependent parameters in our model are calculated from best-fit functions for the climates of the six regions, most of which are measured from monthly average data. These simplified climate models certainly do not capture the full range of temperature fluctuations that take place daily in each region, and the imperfect fit of the Fourier curves in some cases leads to over- or under-reporting of temperatures. In the outdoor simulation for El Paso, for instance, the annual peak vector population is reported to be slightly higher than the equilibrium value for the maximum temperature that the city reaches. This implausible outcome reflects the imprecision of the fundamental temperature equations upon which the model is built.

Beyond the underlying climate functions, our model by nature represents a simplification of the vector lifecycle that does not account for every possible factor influencing population dynamics. We consider death rates in the egg stages to be constant, rather than temperature-dependent, due to a lack of available data describing the effects of temperature on egg viability. In doing so, we likely over-estimate the survival rates of wet and dry eggs in extremely cold conditions: The constant death rates are a probable explanation for our model's prediction of annual re-emergence in Minneapolis under optimal egg flooding conditions. In the larval stages, the density-dependent death rates are calculated based on average field counts and emergence rates over the course of a year (Southwood et al. 1972). These estimates are also imprecise given the age of Southwood's study, its specificity to a particular region of Thailand, and the use of annual averages to determine instar ratios. We introduce additional imprecision in the larval stages by considering temperature-dependent death rates to be equivalent among small larvae, big larvae, and pupae.

Opportunities for further consideration are also present once the vector reaches adulthood. We assume that *Aedes aegypti* adults fall into three categories: feeding, laying, and a third, "post-laying" stage that is relevant to neither disease spread nor oviposition. We make the simplifying assumptions that all females feed for three days before undergoing two oviposition cycles, during which all are able to become gravid. At the end of an egg-laying stage of temperature-dependent length, half of the females return to the feeding stage, while half proceed to the post-egg-laying cohort. The assumptions regarding the length of feeding and number of oviposition cycles are not likely to strictly hold under extreme temperature conditions, signifying that the model is not necessarily representative of adult behavior in all cases. Additionally, our assignment of a constant daily adult death rate, rather than temperature-dependent adult mortality, may lead to an overestimation of the adult population under particularly inhospitable climate conditions.

Finally, there are points of uncertainty in our definition of habitat types and migration patterns. While outdoor, indoor, and enclosed spaces broadly encompass the major habitat types in urban and suburban regions, there exist more distinctions within each habitat than this model can capture. Accounting for differences between shaded and exposed outdoor areas, buildings maintained at different or non-constant temperatures, and enclosed spaces varying from sewers to water towers would require a more detailed set of temperature equations for each habitat and

provide more insight into the effects of habitat heterogeneity. Within our three-habitat structure, the flooding rates and habitat areas that we assign are also based on assumptions, and the effects of variation in these parameters must be considered. The initial flooding rate is calculated assuming that people fill about half of the water containers in their homes and yards about once a week, but these rates stand to vary from household to household given differences in behavior. Furthermore, while we do not consider variations in wetness that arise in regions that are rainier than El Paso, an ideal study would account more explicitly for weather effects in the assignment of flooding rates.

Because it is impossible to measure the total areas of available outdoor, indoor, and enclosed aquatic habitat in each region, we consider various distributions of the three habitats and designate migration rates during oviposition based on the aquatic area falling in each category. We similarly consider vector preferences during feeding by establishing migration rates that are proportional to the number of humans in each environment. However, while these migration rates are logical given the needs of *Aedes aegypti* adults at each stage of the gonotrophic cycle, we lack data to show whether the vector is in fact able to travel at the rates we specify. In further studies of *Aedes aegypti* dispersal, it would be beneficial to consider the potential barriers to migration among manmade habitats. For instance, in the United States, where buildings are typically well-maintained and shielded from their exteriors, migration may be restricted to times at which people open their doors and windows. By contrast, buildings in other regions where the vector is prevalent may include more consistently present openings, allowing for the vector to migrate with higher frequency. In failing to account for the structural soundness of indoor and enclosed spaces, we potentially overstate the extent to which the presence of these habitat types aids the vector's survival.

In spite of the inherent imprecision in our assumptions, the model proposed in this study provides a foundation for understanding *Aedes aegypti* maturation, survival, and migration in urban and suburban areas within and beyond the United States. While estimating the size of the adult *Aedes aegypti* population is only a small step in guiding disease control, in the future, we hope that our system of equations will be paired with a disease dynamics model so as to more closely capture the relationship between population levels and transmission rates. Until then, our model offers a basis for evaluating the vector's range of viability and implies that there exist promising opportunities for vector control through habitat redistribution.

7. References

Bar-Zeev, M. "The effect of temperature on the growth rate and survival of the immature stages of *Aedes aegypti*." *Bull. of Entomol. Research* 49.1 (1958): 157–163.

Barbosa, P., T.M. Peters, and N.C. Greenough. "Overcrowding of mosquito populations: Responses of larval *Aedes aegypti* to stress." *Environ. Ent.* 1 (1972): 89-93.

Barrera, R., M. Amador, and G. Clark. "Use of the pupal survey technique for measuring *Aedes aegypti* (Diptera: Culicidae) productivity in Puerto Rico." *Am. J. Trop. Med. Hyg.* 74.2 (2006): 290-302.

Bouri, N., T.K. Sell, C. Franco, A.A. Adalja, D.A. Henderson, and N.A. Hynes. "Return of epidemic dengue in the United States: Implications for the Public Health Practitioner." *Public Health Rep.* 127.3 (2012): 259-266.

Burke, R., R. Barrera, M. Lewis, T. Kluchinsky, and D. Claborn. "Septic tanks as larval habitats for the mosquitos *Aedes aegypti* and *Culex quinquefasciatus* in Playa-Playita, Puerto Rico." *Med. Vet. Entomol.* 24 (2010): 117-123.

Chan, K.L., B.C. Ho, and Y.C. Chan. "*Aedes aegypti* and *Aedes albopictus* in Singapore City." *Bull. World Health Org.* 44 (1971): 629-633.

"Chikungunya." *Centers for Disease Control and Prevention*, Centers for Disease Control and Prevention, 29 Aug. 2017, www.cdc.gov/chikungunya/index.html.

Christophers, S. "*Aedes aegypti* (L.) the yellow fever mosquito: its life history, bionomics and structure." (1960).

Costa, E.A., E. Santos, J.C. Correia, and C. Albuquerque. "Impact of small variations in temperature and humidity on the reproductive activity and survival of *Aedes aegypti* (Diptera: Culicidae)." *Revista Brasileira de Entomologia.* 54.3 (2010): 488-493.

"Dengue." *Centers for Disease Control and Prevention*, Centers for Disease Control and Prevention, 19 Jan. 2016, www.cdc.gov/dengue/index.html.

Diffey, B. L. "An overview analysis of the time people spend outdoors." *British Journal of Dermatology* 164.4 (2011): 848-854.

Dye, C. "Models for the population dynamics of the Yellow Fever mosquito, *Aedes aegypti*." *J. Animal Ecol.* 53.1 (1984): 247-268.

Edman, J. D., et al. "Aedes aegypti (Diptera: Culicidae) movement influenced by availability of oviposition sites." *Journal of Medical Entomology* 35.4 (1998): 578-583.

- Eisen, L., A.J. Monaghan, S. Lozano-Fuentes, D.F. Steinhoff, M.H. Hayden, and P.E. Bieringer. "The impact of temperature on the bionomics of *Aedes (Stegomyia) aegypti*, with special reference to the cool geographic range margins." *J. Med. Entomol.* 51.3 (2014): 496-516.
- Ermert, V., A.H. Fink, A.E. Jones, and A.P. Morse. "Development of a new version of the Liverpool Malaria Model. I. Refining the parameter settings and mathematical formulation of basic processes based on a literature review." *Malaria Journal.* 10.35 (2011).
- Faull, K.J., and C.R. Williams. "Intraspecific variation in desiccation survival time of *Aedes aegypti* (L.) mosquito eggs of Australian origin." *Journal of Vector Ecology* 40.2 (2015): 292-300.
- Focks, D.A., D.G. Haile, E. Daniels, and G.A. Mount. "Dynamic life table model for *Aedes aegypti* (Diptera: Culcidae): analysis of the literature and model development." *J. Med. Entomol.* 30.6 (1993): 1003-1017.
- Gilpin, M.E., G.A.H. McClelland, and J.W. Pearson. "Space, time, and the stability of laboratory mosquito populations." *The American Naturalist* 110.976 (1976): 1107-1111.
- Judson, C. "Feeding and oviposition behavior in the mosquito *Aedes aegypti*. I. Preliminary studies of physiological control mechanisms." *Biological Bulletin* 133.2 (1967): 369-377.
- Klowden, M.J. and H. Briegel. "Mosquito gonotrophic cycle and multiple feeding potential: contrasts between *Anopheles* and *Aedes* (Diptera: Culcidae)." *Journal of Medical Entomology.* 31.4 (1994): 618-622.
- Magori, K., M. Legros, M.E. Puente, D.A. Focks, T.W. Scott, A.L. Lloyd, and F. Gold. "Skeeter Buster: A stochastic, spatially explicit modeling tool for studying *Aedes aegypti* population replacement and population suppression strategies." *PLoS Neglected Tropical Diseases* 3.9 (2009): e508.
- McDonald, P.T. "Population characteristics of domestic *Aedes aegypti* (Diptera: Culicidae) in villages on the Kenya Coast I. Adult survivorship and population size." *Journal of Medical Entomology* 14.1 (1977): 42-48.
- Monaghan, A.J., et al. "On the seasonal occurrence and abundance of the Zika virus vector mosquito *Aedes aegypti* in the contiguous United States." *PLoS Currents* (2016): 8.
- Moore, C.G., and D.M. Whitacre. "Competition in mosquitos: Production of *Aedes aegypti* larval growth retardant at various densities and nutrition levels." *Ann. Entomol. Soc. Am.* 65.4 (1972): 915-918.
- Naylor, S. and A. Gustin. "Geothermal ground source heat pumps and geology in Indiana." *Indiana Geological Survey.* 2017.

- Pant, C.P. and M. Yasuno. "Field studies on the gonotrophic cycle of *Aedes aegypti* in Bangkok, Thailand." *J. Med. Entomol.* 10.2 (1973): 219-223.
- Ritchie, S.A., B.L. Montgomery, and A.A. Hoffman. "Novel estimates of *Aedes aegypti* (Diptera: Culicidae) population size and adult survival based on *Wolbachia* releases." *J. Med. Entomol.* 50.3 (2013): 624-631.
- Rueda, L.M., K.J. Patel, R.C. Axtell, and R.E. Stinner. "Temperature-dependent development and survival rates of *Culex quinquefasciatus* and *Aedes aegypti* (Diptera: Culicidae)." *J. Med. Entomol.* 27.5 (1990): 892-898.
- Russell, B. M., B. H. Kay, and W. Shipton. "Survival of *Aedes aegypti* (Diptera: Culicidae) eggs in surface and subterranean breeding sites during the northern Queensland dry season." *Journal of Medical Entomology* 38.3 (2001): 441-445.
- Sharpe, P. J. H. & D. W. DeMichele. "Reaction kinetics of poikilotherm development." *J. Theor. Biol.* 64 (1977): 649-670.
- Sheppard, P.M., W.W. McDonald, R.J. Tonn, and B. Grab. "The dynamics of an adult population of *Aedes aegypti* in relation to Dengue Haemorrhagic Fever in Bangkok." *J. Animal Ecol.* 38.3 (1969): 661-702.
- Southwood, T.R.E., G. Murdie, M. Yasuno, R.J. Tonn, and P.M. Reader. "Studies on the life budget of *Aedes aegypti* in Wat Samphaya, Bangkok, Thailand." *Bull. World Health Org.* 46 (1972): 211-226.
- Sota, T., and M. Mogi. "Interspecific variation in desiccation survival time of *Aedes (Stegomyia)* mosquito eggs is correlated with habitat and egg size." *Oecologia* 90 (1992): 353-358.
- Tinti, F., A. Barbaresi, S. Benni, D. Torreggiani, R. Bruno, and P. Tassinari. "Experimental analysis of thermal interaction between wine cellar and underground." *Energy and Buildings* 104 (2015): 275-286.
- Troyo, A., O. Calderón-Arguedas, D.O. Fuller, M.E. Solano, A. Avendaño, K.L. Arheart, D.D. Chadee, and J.C. Beier. "Seasonal profiles of *Aedes aegypti* (Diptera: Culicidae) larval habitats in an urban area of Costa Rica with a history of mosquito control." *J. Vector Ecol.* 33.1 (2008): 76-88.
- Tun-Lin, W., T.R. Burkot, and B.H. Kay. "Effects of temperature and larval diet on development rates and survival of the dengue vector *Aedes aegypti* in north Queensland, Australia." *Med. Vet. Entomol.* 14 (2000): 31-37.
- Visvanathan, C., S. Vigneswaran, and J. Kandasamy. "Rainwater Collection and Storage in Thailand: Design, Practices and Operation." *Journal of Water Sustainability* 5.4 (2015): 129-139.

Wallace, D., O. Prosper, J. Savos, A. Dunham, J. Chipman, X. Shi, B. Ndenga, and A. Githeko. "Modeling the Response of *Anopheles gambiae* populations in the Kenya highlands to a rise in mean annual temperature." *J. Med. Entomol.* 54.2 (2017): 299-311.

Watts, D. "Re: *Aedes aegypti* project." Message to Annika Roise and Dorothy Wallace. 20 Sept. 2017. E-mail.

Yang, H.M., M.L.G. Macoris, K.C. Galvani, M.T.M. Andrighetti, and D.M.V. Wanderley. "Assessing the effects of temperature on the population of *Aedes aegypti*, the vector of dengue." *Epidemiol. Infect.* 137.8 (2009): 1188-1202.

"Yellow Fever." *Centers for Disease Control and Prevention*, Centers for Disease Control and Prevention, 4 Apr. 2018, www.cdc.gov/yellowfever/index.html.

"Zika Virus." *Centers for Disease Control and Prevention*, Centers for Disease Control and Prevention, 29 Sept. 2016, <https://www.cdc.gov/zika/about/index.html>.

"Zika Virus Fact Sheet." *World Health Organization*, World Health Organization, 8 Feb. 2018, <http://www.who.int/en/news-room/fact-sheets/detail/zika-virus>.